How the Blue Economy affects plankton dynamics in the Belgian part of the North Sea:

a modeling approach

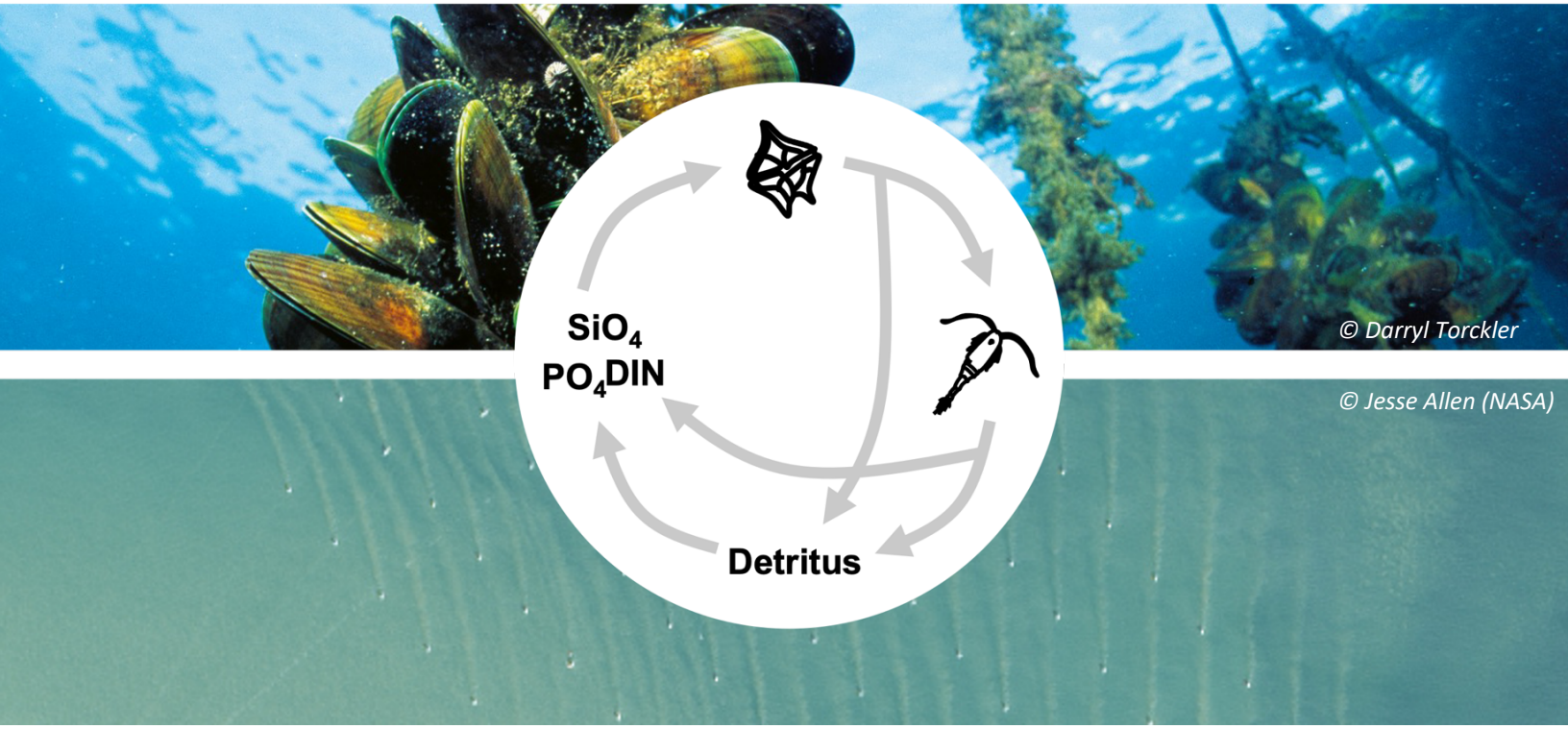

Martha Stevens

Promotors: Prof. Dr. Marleen De Troch
Dr. Ir. Gert Everaert

Supervisor: Steven Pint

Academic year: 2022 – 2023

A dissertation submitted to Ghent University in partial fulfillment of the requirements for the degree of International Master of Science in Marine Biological Resources (IMBRSea).

GHENT UNIVERSITY IMBRSea VLIZ

The effects of blue economy activities on plankton biomass dynamics in the Belgian part of the North Sea: a modeling approach

Executive summary

Planktonic organisms play a crucial role in marine food webs and are known drivers of biogeochemical cycles. In addition to these ecosystem services, marine plankton can affect industries in the blue economy directly, for example by impacting fisheries yield. However, economic activities themselves can alter the marine environment in such a way that plankton dynamics are affected. Mussel aquaculture, for instance, introduces additional grazing pressure and can alter nutrient fluxes, whereas offshore wind turbines are known to be associated with turbid plumes. The Belgian Part of the North Sea (BPNS) is an excellent study area to investigate how activities in the blue economy might affect local plankton dynamics due to its variety of active industries and high data coverage. In this thesis, a Nutrient-Phytoplankton-Zooplankton-Detritus (NPZD) model was used to describe local phyto- and zooplankton dynamics and simulate the effects of two hypothetical scenarios: the introduction of mussel aquaculture and an offshore wind farm. The model had been previously calibrated to accurately describe plankton dynamics in the BPNS. It calculates daily phyto- and zooplankton biomass based on time-series input data on nutrient concentrations, sea surface temperature (SST) and solar irradiance. After an extensive literature review, model input and parameters were adjusted to reflect the environmental changes associated with each scenario (i.e. changed nutrient concentrations, grazing rate, and turbidity). These effects were first explored individually by calculating phyto- and zooplankton biomass response curves for each scenario. Then, the model was used to simulate plankton dynamics for both scenarios. Finally, the scenarios were compared to current plankton dynamics in the BPNS. According to model predictions, the introduction of mussel aquaculture would be associated with severe phyto- and zooplankton depletion ranging from 96.5% to 99.9% depending on the time of year. Whereas offshore wind farms would increase median yearly phytoplankton biomass by 50.5% and decrease yearly zooplankton biomass by 95.3%. Additionally, seasonal patterns shifted from three yearly blooms towards two. These results suggest that commercial activities in the BPNS have the potential to alter plankton dynamics significantly. This thesis highlights the need for increased monitoring efforts concerning the environmental effects of economic developments, as well as the possibility of using modeling as a tool to assist policy makers in the permitting and spatial planning of commercial activities in the BPNS.

Abstract

Planktonic organisms drive biogeochemical cycles and play a crucial role in marine food webs. Additionally, marine plankton can directly or indirectly affect industries in the blue economy. However, economic activities themselves can alter the marine environment so that plankton dynamics are affected. A Nutrient-Phytoplankton-Zooplankton-Detritus (NPZD) model was used to describe phyto- and zooplankton dynamics in the BPNS and simulate the effects of two economic developments: mussel aquaculture and an offshore wind farm. According to model predictions, introducing mussel aquaculture in the BPNS would cause severe phyto- and zooplankton depletion with biomass declines ranging from 96.5% to 99.9% depending on the time of year. Whereas offshore wind infrastructure would increase median yearly phytoplankton biomass by 50.5% and decrease yearly zooplankton biomass by 95.3%. Additionally, seasonal patterns changed, with a shift from three yearly blooms towards two. It can thus be concluded that commercial activities in the BPNS have the potential to significantly alter plankton dynamics. Modeling approaches such as applied in this thesis, in addition to increased monitoring efforts, can be a valuable tool to assist policy makers decision-making concerning permitting and spatial planning of economic activities in the BPNS.

Visual abstract

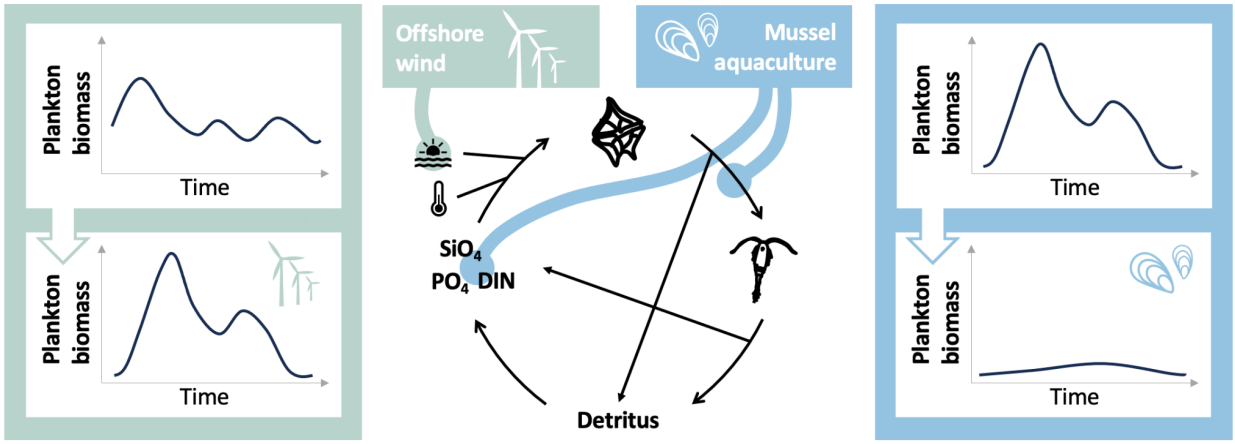

1. Introduction

Marine phytoplankton is responsible for approximately 50% of global primary production and forms the base of marine food webs (Field et al., 1998). Moreover, both phyto- and zooplankton are important drivers of various biogeochemical cycles (Cavan et al., 2017; Litchman et al., 2015). In addition to these ecosystem services, marine plankton directly affects the blue economy in multiple ways. Phytoplankton can for example be used to produce biofuels, and it is a valuable source of bioactive ingredients and genetic resources (Naselli-Flores & Padisák, 2022). Planktonic primary production also impacts fisheries yields (Chassot et al., 2010), enabled by the transfer of energy by herbivorous zooplankton to higher trophic levels (Lomartire et al., 2021; Sterner, 2009).

Because of its clear biological, societal, and economic importance, a deep understanding of plankton dynamics is crucial. According to Liebig's law of the minimum, phytoplankton growth is restricted by the least available resource in the environment (De Baar, 1994). However, plankton dynamics are usually more complex, with primary production being determined by co-limitation of resources (Harpole et al., 2011). In the North Sea, the main limiting factors are nutrients, solar irradiance, and sea surface temperature (Blauw et al., 2018). Along with these bottom-up restraints, phytoplankton biomass and species composition are regulated by zooplankton grazing (Welschmeyer & Lorenzen, 1985). Seasonal variability in these environmental and biological controls results in the annual plankton cycle observed in temperate regions. High nutrient availability combined with sufficient solar irradiance in autumn and spring lead to two seasonal phytoplankton blooms, each followed by zooplankton bloom and a period of increased grazing pressure (Irigoien et al., 2005). As a result of continuously changing environmental conditions, both phyto- and zooplankton biomass vary at a high-resolution spatiotemporal scale (Otero et al., 2022). In addition to this natural variation, anthropogenic activities can directly or indirectly alter the marine environment (Halpern et al., 2007), thereby affecting plankton dynamics. A well-described example of human activities indirectly altering the marine environment is anthropogenic climate change, resulting in ocean warming (IPCC, 2021). Linked to these increased sea surface temperatures (SST) regional changes in primary productivity have been observed (Käse & Geuer, 2018), as well as shifts in zooplankton community structure (Heneghan et al., 2023). In coastal ecosystems, direct anthropogenic stressors such as fishing, shipping, and other economic activities, add to pressure caused by climate change (Moser et al., 2012; Rockström et al., 2009).

The Belgian part of the North Sea (BPNS) is a prime example of a coastal area that has been impacted heavily by both climate change and local human activities. The SST in the BPNS has risen by approximately 1°C since 1970 (Lagring et al., 2018) and nutrient concentrations are strongly defined by riverine inputs from continental Europe through the river Scheldt, the Seine, Rhine, and Meuse (Lacroix et al., 2007). Varying nutrient availability due to land-use changes, as well as the increased SST and a decrease in turbidity have caused changes in phytoplankton composition, biomass, and seasonality in the BPNS throughout the last 50 years (Nohe et al., 2020). On top of that, the BPNS is an economically valuable area with a wide variety of activities ranging from tourism to fisheries and sand-extraction in a small area of just 3,454 km² (Dauwe et al., 2022). This accumulation of anthropogenic influences could further alter plankton dynamics, impacting the marine ecosystem as well as the societal and economical services they provide (Doney et al., 2012). The BPNS is an excellent study area to investigate the effects of economic

activities on plankton dynamics because in addition to its many stakeholder uses, there are long-term observations available with high spatial resolution (Dauwe et al., 2022; Mortelmans et al., 2019a).

The Belgian blue economy is continuously evolving, with a multitude of plans and developments ahead that might impact local plankton dynamics. One example is the recent development of the first commercial mussel farm in the BPNS, with plans for its expansion already approved (Dauwe et al., 2022). The following increased abundance of filter feeders might affect plankton dynamics through a variety of pathways. For example, mussels regulate phytoplankton growth through bottom-up effects by adapting nutrient and oxygen fluxes (Nizzoli et al., 2011; Richard et al., 2006), as well as through top-down effects by mussel grazing (Cugier et al., 2010). This alters prey abundance for zooplankton, affecting their biomass and species composition (Nielsen & Maar, 2007). Depending on environmental conditions, mussel grazing can also directly control zooplankton communities through the removal of pelagic competitors (Maar et al., 2007; Nielsen & Maar, 2007). Another growing industry in the Belgian blue economy is renewable energy production. Currently, 238 km^2 of the BPNS is covered by offshore wind farms, with a supplementary 281 km^2 assigned for additional offshore wind developments (Dauwe et al., 2022). When these new projects are finished roughly $1/7^{th}$ of the BPNS will be covered by wind turbines. Offshore wind farms and their effects on marine ecosystems have been extensively monitored and studied but this research often focused on benthic ecosystems, birds, or marine mammals (Degraer et al., 2020a; Degraer et al., 2020b). However, some recent studies have highlighted the potential effects of offshore wind farms on regional primary productivity (Slavik et al., 2017). Increased turbulence at the base of turbines can be associated with increased vertical mixing, which affects thermal regimes and transports nutrients to the surface (Floeter et al., 2017). Additionally, turbines are known to produce suspended particulate matter (SPM) plumes that can be up to several kilometers in length (Vanhellemont & Ruddick, 2014). Although the origin of these plumes remains unclear, current hypotheses include increased bottom scouring or sediment resuspension at piles, as well as detritus from biofouling organisms (Baeye & Fettweis, 2015; Forster, 2018). The reduction of light availability in these plumes could lead to decreased phytoplankton growth. To date, insight into the effects of environmental changes on local plankton dynamics caused by blue economy activities in the BPNS remains limited.

The complex effects of environmental changes on plankton dynamics can be explored using ecological modeling. This approach allows the integration of a wide range of biological and environmental data into a holistic mechanism for understanding plankton dynamics. Previous studies have used ecological models to predict and assess the impact of events such as oil spills or hurricanes (Davenport et al., 2012; González et al., 2022).

The goal of this master thesis is to quantify the effects of mussel aquaculture and offshore wind farms on plankton biomass dynamics in the BPNS through scenario-based analyses. Possible environmental effects of these developments are inferred from literature and incorporated into a Nutrient-Phytoplankton-Zooplankton-Detritus (NPZD) model. The outcome of this thesis provides new insights into the impact of the blue economy on the pelagic ecosystem of the BPNS and could be used to inform future management practices.

2. Materials and Methods

An NPZD model was used to quantify the effects of economic activities in the BPNS on local plankton dynamics. To do so, a three-step approach was implemented. First, two hypothetical scenarios were developed, inspired by the future development of offshore wind farms and mussel aquaculture. Based on an extensive literature review concerning these two economic activities, this study focused on three variables. Nutrient concentrations (i.e. dissolved inorganic nitrate (DIN), PO_4 and SiO_4) and mussel grazing were taken into account for the mussel aquaculture scenario, and turbidity was studied in the offshore wind scenario. Depending on how a variable was incorporated into the model, either the input data, parameter values or the model itself were adapted to simulate its effects on plankton dynamics. Secondly, the effects of changes in each individual variable on phyto- and zooplankton biomass were explored by calculating plankton biomass response curves. A classic example of a response curve is the Monod equation, which describes the relationship between microbial growth and the concentration of a limiting nutrient in their environment (Monod, 1949). In this thesis, the same principles were applied to describe how plankton biomass relates to changes in the availability of each studied variable. Finally, the effect of offshore wind farms and mussel aquaculture on plankton dynamics in the BPNS was quantified. To achieve this, baseline plankton dynamics were compared to those predicted by the model for each blue economy scenario.

2.1 Study area and data

Based on the marine spatial plan (MSP) for the BPNS (Verhalle & Van de Velde, 2020) two areas of interest were identified for a mussel aquaculture site and an offshore wind farm (Figure 1). These are located in the nearshore and offshore regions respectively, for which the model had been previously optimized to simulate local plankton dynamics by Otero et al. (2022). Both regions include LifeWatch stations, where the biotic and abiotic environment are monitored regularly as a part of the European Research Infrastructure within the European Strategy Forum on Research (ESFRI) (Mortelmans et al., 2019a; Mortelmans et al., 2019b). Nearshore stations are sampled monthly, whereas offshore stations are visited seasonally. Because of its location in the nearshore area, station 130 was used as a baseline to study the potential effects of mussel aquaculture. For the offshore region associated with wind farms, data from all available LifeWatch stations was combined to account for the lower sampling rate in this region.

Specifically, two open-access datasets from LifeWatch were used for this master thesis. The first dataset contains zooplankton abundances obtained through Zooscan analysis (Mortelmans et al., 2019b; VLIZ, 2023). Note that only data from selected taxa (i.e. Calanoida, Noctiluca, Harpacticoida and Appendicularia) was included. These taxa account for 76% of the total zooplankton density (Van Ginderdeuren et al., 2014) and can accurately represent the main biomass dynamics of zooplankton in the BPNS. The second dataset contained nutrient concentrations with measurements conducted by a Skalar Autoanalyser system, as well as *in situ* pigment concentrations performed by HPLC, and SST measured by CTD (Mortelmans et al., 2019a; VLIZ, 2021).

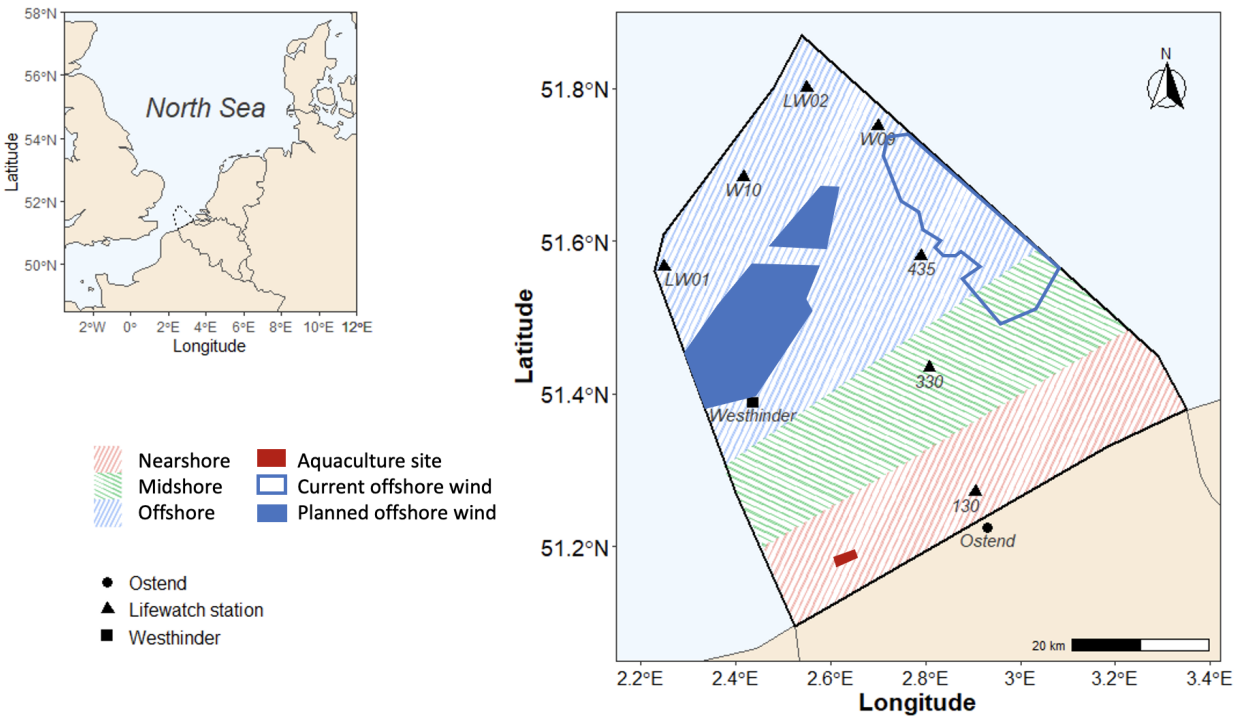

Figure 1: *Map of the BPNS highlighting the near- to offshore regions as well as the location of current and planned offshore wind and aquaculture sites. Additionally, all LifeWatch stations that were consulted for this master thesis, as well as the Westhinder station are marked.*

To infer daily time series for SST and nutrient concentrations required as model input, a higher temporal coverage than provided by LifeWatch campaigns was needed. For this reason, additional datasets from the Westhinder buoy and station run by the Flemish Banks Monitoring Network were consulted (IVA MDK, n.d.). Due to substantial gaps in the Westhinder SST dataset in 2018, a subset from 2014 to 2017 was used. This data had been previously compiled into two datasets appropriate for the NPZD model by Pint and Otero (2022).

2.2 NPZD model

Phyto- and zooplankton biomass dynamics in the BPNS were simulated with an NPZD model created by Soetaert & Herman (2009) and subsequently adapted by Everaert et al. (2015) and Otero et al. (2022). This closed ecosystem model describes the relationships between four state variables (nutrients, phytoplankton, zooplankton, and detritus) influenced by two forcing functions (solar irradiance and SST) (Figure 2) (Appendix A). For each time-step the model is expressed in mmol N m^{-3} day^{-1}. As input data, daily time series for nutrient concentrations (i.e. DIN, PO_4 and SiO_4), SST, and solar irradiance were assembled. For nutrients and SST these time series were created based on the Westhinder dataset (see section 2.1) using general additive models. Solar irradiance on the other hand, is modeled as photosynthetically active radiation (PAR) which is surface irradiation corrected with the diffuse attenuation coefficient (Kd), i.e. accounting for light diminishing with depth due to turbidity, based on the Lambert-Beer law (Kirk, 1994; Lund-Hansen, 2004). The effects of both PAR and nutrient concentrations

on phytoplankton growth are described by Michaelis-Menten equations (Soetaert & Herman, 2009). The effect of SST is described by a Thomann and Mueller equation (Thomann & Mueller, 1987). Model calculations are based on thirteen parameters for which seasonal minimum and maximum values were defined by Otero et al. (2022) to optimally mimic the biogeochemical processes in the BPNS. All model calculations were performed in R (R Core Team, 2022; version 4.2.1) (Appendix A).

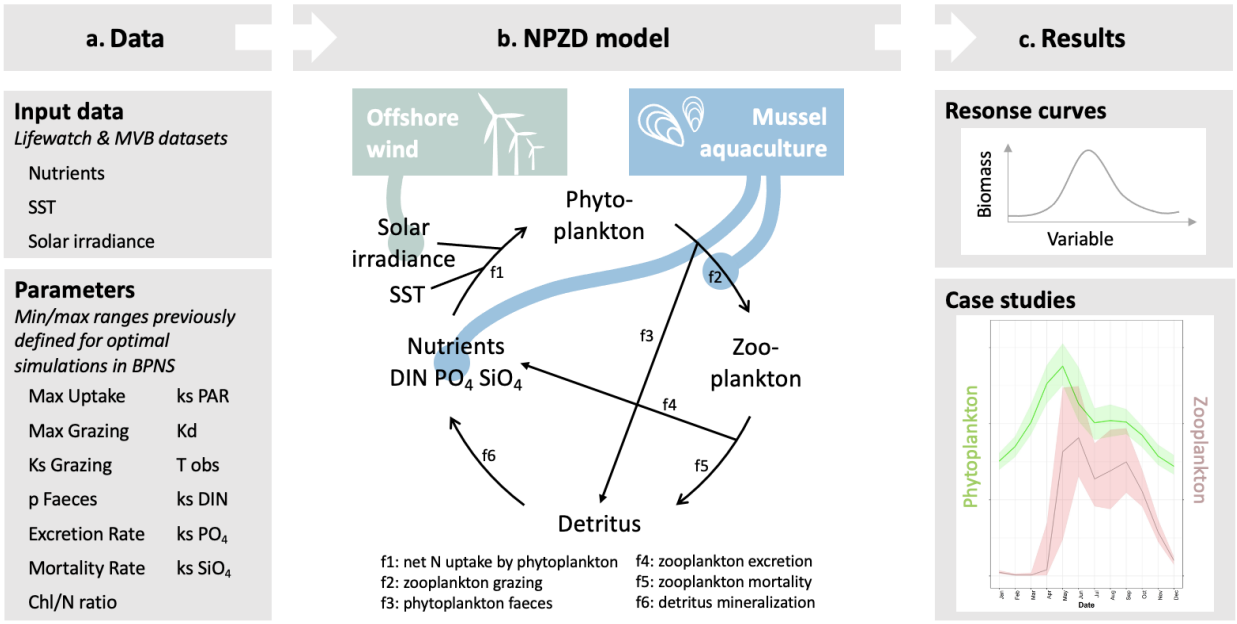

Figure 2: *Workflow and use of the NPZD model. From left to right: (a.) Data and parameters incorporated in the model. (b.) Overview of the NPZD model and the flows between state variables (f1-f6). The variables affected by the offshore wind and aquaculture scenarios are highlighted in green and blue, respectively. (c.) The expected outcome from the model calculations: a phyto- and zooplankton biomass response curve for each selected variable and the yearly plankton dynamics for each scenario.*

2.3 Scenarios

To quantify the effects of blue economy activities in the BPNS, a scenario-based approach was implemented. First, the NPZD model was used to simulate plankton dynamics in the near- and offshore region of the BPNS under present circumstances from 2014-2017 (i.e. baseline scenarios). Subsequently, these baselines were compared to two hypothetical scenarios concerning mussel aquaculture and offshore wind farms.

2.3.1 Near- and offshore baseline

To create two baseline scenarios, the calibrated model was run in 5000 iterations with random parameter values for both the nearshore and offshore region to simulate plankton biomass dynamics from 2014-2017. These parameter values were selected within a realistic range for the near- and offshore regions respectively, which was previously determined by Otero et al. (2022). Next, the simulations were validated by comparison to observed phyto- and zooplankton biomass from LifeWatch campaigns in their respective region during the study period. The root mean squared error (RMSE) was calculated to evaluate model fit.

This measure was used to assess the difference between predicted and observed plankton biomass, and is described by the following equation (Eq. 1):

$$RMSE = \sqrt{\frac{\sum_{i=1}^{N}(Predicted_i - Observed_i)^2}{N}} \quad \text{(Eq. 1)}$$

The 10% best simulations (i.e. those with the smallest RMSE) were selected. These best simulations were used as baseline plankton dynamics for the near- and offshore regions.

2.3.2 Mussel aquaculture

The mussel aquaculture scenario was based on the dynamics in the nearshore region and defined by changes in two drivers of plankton dynamics: nutrient concentrations and mussel grazing (Table 1). First, the bottom-up effect of changed nutrient fluxes due to mussel nutrient recycling was considered. Specifically, mussel presence was assumed to be a net nutrient source with high seasonal variability (Table 2) (Nielsen & Maar, 2007; Nizzoli et al., 2011; Richard et al., 2006). Second, the top-down effect of mussel grazing on phytoplankton was included as a constant grazing increase equal to 50% of zooplankton grazing in summer based on findings from Jacobs et al. (2015). Mussel grazing on zooplankton was considered insignificant in comparison and thus not included in this scenario. Mussel valve closure at extremely low (0.5 mgL^{-1}) and high (8 mgL^{-1}) chlorophyll concentrations was also accounted for (Lüskow & Riisgård, 2018).

First, the effects of changes in individual variables (i.e. nutrient concentrations and mussel grazing) on plankton dynamics were explored by calculating plankton biomass response curves. This was achieved by running a series of model iterations where all parameters and input data remained at their baseline values, except for the variable of interest. The parametrization used was a fixed set of optimal values from the single best simulation for the nearshore region based on a calibrated and validated NPZD model by Otero et al. (2022) (Table 1). To calculate the plankton biomass response to changes in nutrient concentrations, the baseline input data for DIN, PO_4 and SiO_4 was multiplied with a range of factors (0, 0.1, 0.2, …, 10) creating three new sets of input data. For each new set, a model iteration was run for every multiplication factor, thus simulating a range of changes to the nutrient concentrations. Note that for the purpose of calculating these response curves, a constant multiplication was applied throughout the entire input data set, not taking the previously described seasonal variation in nutrient flux adaptations into account. Instead, for each nutrient the maximal concentration increase observed throughout the year was studied (Table 2) (Nielsen & Maar, 2007; Nizzoli et al., 2011). For example, DIN was increased by 200% (i.e. the maximal change observed in spring) throughout the year (Table 2). Next, to simulate a range of grazing rates, a multiplication factor was added to the grazing equation. The model was then run in a series of iterations where for each this multiplication factor varied in a set range of values (0, 0.1, 0.2, …, 10). As for the nutrients, in this case a constant increase was applied throughout the year, not taking valve closure at certain chlorophyll concentrations into account. These simulations, for ranges of grazing rates and nutrient concentrations, were then used to calculate and visualize the phyto- and zooplankton biomass responses to the individual environmental changes associated with offshore wind farms.

Table 1: *Set of optimal parameter values for the nearshore region based on a calibrated and validated NPZD model by Otero et al. (2022)*

	Nearshore region Mussel aquaculture	
Parameters	Spring	Fall
Max uptake	0.727	0.583
ks PAR	176	205
ks DIN	3.287	1.896
ks P	0.324	0.346
ks Si	0.599	0.573
Max grazing	0.893	0.887
Ks grazing	2.267	1.610
p Faeces	0.362	0.370
Excretion rate	0.160	0.163
Mortality rate	0.307	0.349
Chl:N ratio	7.807	7.619
T obs	9.978	10.262
Kd	0.859	0.790

Finally, the combined effects of changes in nutrient concentration and grazing rates on plankton dynamics were studied by incorporating both into the model. Nutrient concentrations were increased in the input data to mimic the seasonal changes in nutrient fluxes associated with mussel aquaculture (Table 2) (Nielsen & Maar, 2007; Nizzoli et al., 2011; Richard et al., 2006). The increased phytoplankton grazing associated with mussel presence was introduced into the model calculations itself by increasing the zooplankton state variable in the grazing equation with a constant value representing mussel biomass (0.081 mmol N m^{-3}) (Appendix A). This value equals half of the mean zooplankton biomass in the nearshore region in summer, as Jacobs et al. (2015) found a 50% increase in phytoplankton grazing due to mussel presence in this season. A 'if-else' function ensured that no additional grazing occurred whenever chlorophyll concentrations fell outside the filtration range of 0.5-8 mgL^{-1} (Lüskow & Riisgård, 2018). For this adjusted model 5000 iterations were run with parameter values randomly selected within a realistic range for the nearshore region previously determined by Otero et al. (2022). All of these simulations were used for further analysis, instead of selecting the best models based on the RMSE since this was a hypothetical scenario and no *in situ* data was available in the BPNS for comparison.

Table 2: *Environmental and biological effects of mussel aquaculture*

Case study	**Variable**	**Expected changes**					**Literature**
Mussel Aquaculture	Nutrients		winter	spring	summer	fall	Nizzoli et al. (2011) Nielsen & Maar (2007)
		DIN	+100%	+200%	+100%	no	
		PO_4	+40%	+20%	+8%	change	
		SiO_4	+25%	+50%	+25%		
	Grazing	Chla < 8μg/L: +0,081 mmolN m^{-3} mussel biomass					Lüskow & Riisgård (2018) Jacobs et al. (2015)
		Chla > 8μg/L: no additional grazing					

2.1.3 Offshore wind farm

The offshore wind farm scenario focused on increased turbidity due to SPM plumes associated with wind turbines and used plankton dynamics in the offshore region of the BPNS as its foundation. A 43% increase in the diffuse attenuation coefficient (Kd) was assumed based on SPM measurements in offshore wind farms (Forster, 2018) and the relationship between SPM and Kd (Devlin et al., 2008) (Table 1). Thermal regimes and nutrient availability could also be affected due to increased vertical mixing at turbines, but this was considered negligible in the BPNS because of its well-mixed waters (Lacroix et al., 2007). Grazing effects by biofouling organisms were not included either, because in comparison to the kilometers-long SPM plumes, the scale of their effect was considered insignificant.

Similar to the aquaculture scenario, first the effects of changes in turbidity on plankton dynamics were explored by calculating plankton biomass response curves. The parametrization in this scenario was a fixed set of optimal values from the offshore region (Otero et al., 2022) (Table 3). Several parameter sets were created where each value remained constant, except for Kd, which was multiplied with a range of factors (0, 0.05, 0.10 …, 5). For each new parameter set a model iteration was run, resulting in a range of simulations showing the effect of different Kd values on phyto- and zooplankton biomass.

Table 3: *Set of optimal parameter values for the offshore region based on a calibrated and validated NPZD model by Otero et al. (2022)*

	Offshore region Offshore wind farms	
Parameters	Spring	Fall
Max uptake	0.536	0.419
ks PAR	186	182
ks DIN	2.367	2.796
ks P	0.427	0.394
ks Si	0.494	0.666
Max grazing	0.880	0.901
Ks grazing	1.754	1.216
p Faeces	0.280	0.298
Excretion rate	0.122	0.114
Mortality rate	0.352	0.322
Chl:N ratio	7.038	4.329
T obs	11.955	13.060
Kd	0.298	0.357

Finally, the effect of offshore wind farms on plankton dynamics was quantified. To achieve this, 5000 model iterations were run with random parameter values within a realistic range for the offshore region determined by Otero et al. (2022). Based on *in situ* SPM measurements in the turbid wake of offshore wind turbines, the range of the Kd parameter was shifted upwards with 43% (Table 4) (Devlin et al., 2008; Forster, 2018). Since the findings from this hypothetical scenario could not be validated by *in situ* data, all simulations were used for comparison to the baseline scenario.

Table 4: *Environmental and biological effects of offshore wind*

Case study	Variable	Expected changes	Literature
Offshore Wind	Turbidity	Kd parameter range +43%	Forster (2018) Devlin et al. (2008)

2.4.1 Statistical analysis

Due to model spin-up time, only simulated biomass from 2015-2017 was used for further analysis (Appendix B). Phyto- and zooplankton biomass for each scenario were tested with a Shapiro-Wilk test ($p > 0.05$), from which it was concluded that the data was not distributed normally. Hence, potential differences in phyto- and zooplankton biomass between scenarios were tested using the non-parametric Wilcoxon rank sum test. All statistical analyses were performed using the package 'stats' in R (R Core Team, 2018).

3. Results

3.1 Mussel aquaculture

3.1.1 Response curves

An NPZD model was used to create phytoplankton and zooplankton biomass response curves for variables related to mussel aquaculture, i.e. changes in nutrient concentrations and grazing rate. When the concentrations for all nutrients were increased simultaneously, a steady rise in both phyto- and zooplankton biomass was predicted until an eventual model collapse from a 90% nutrient increase onwards (Figure 3a,c). Throughout this rise, seasonal phytoplankton dynamics remained constant (Figure 3b). However, the maximal seasonal zooplankton biomass shifted from summer towards spring when the nutrient increase exceeded 30% (Figure 3d). With declining nutrient availability, zooplankton disappeared almost completely ($1.12*10^{-41}$ mmol N m^{-3}), whereas phytoplankton biomass reached a minimum of 3.63 mg Chl m^{-3}. This phytoplankton biomass decrease was associated with strong seasonal shifts: the regular spring phytoplankton bloom gave way to a summer bloom (Δnutr. = -60%), fall bloom (Δnutr. = -80%), and eventually another summer bloom (Δnutr. = -90%) (Figure 5b). These shifts were reflected in the maximal zooplankton biomass which shifted from summer to fall (Δnutr. = -40%), and back to summer (Δnutr. = -60%) until zooplankton depletion was reached (Figure 3d).

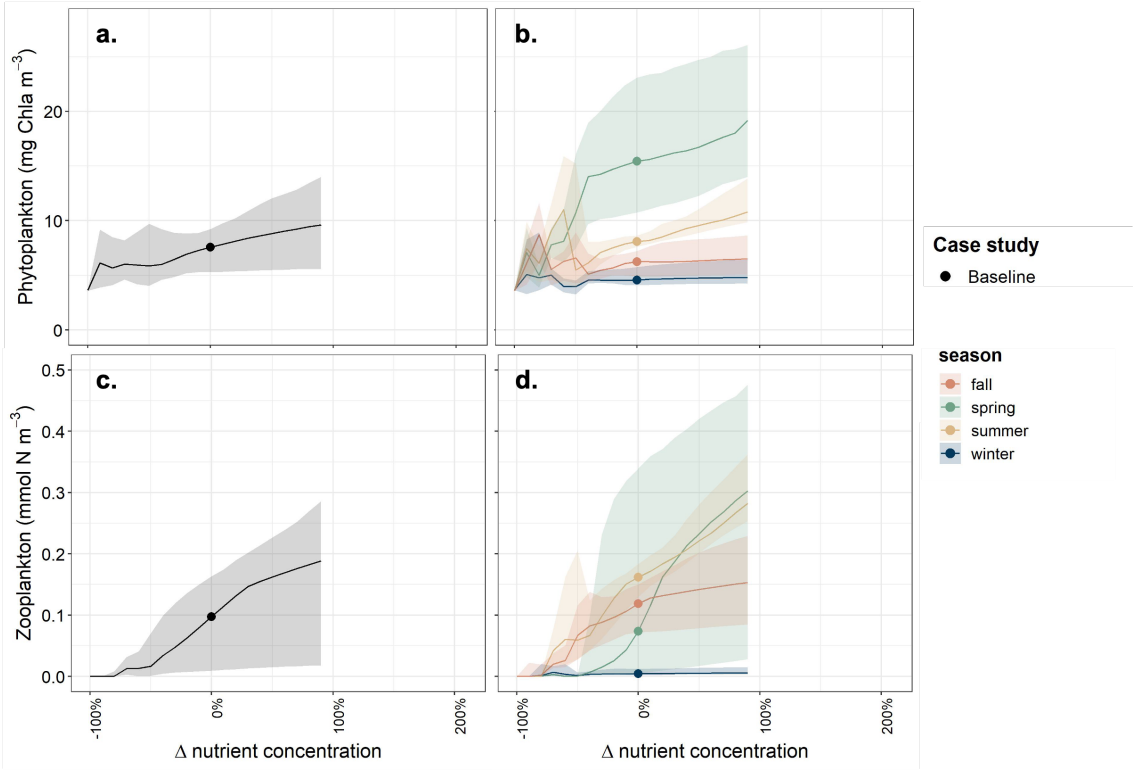

Figure 3: *Response of phytoplankton (a, b) and zooplankton (c, d) biomass to changes in nutrient concentration. Gray curves represent median biomass overall, whereas colored curves represent seasonal median biomass. For each curve the interquartile range is marked as well. The biomass where nutrient concentrations are at nearshore baseline values is marked with a dot.*

The calculation of response curves for individual nutrient changes related to mussel aquaculture was used to quantify their separate effects on plankton biomass (Figure 4). A constant 200% increase of DIN throughout the year resulted in a 7.3% (W = 972894, p = p < 0.001) overall rise in phytoplankton biomass (Table 5), along with a 31.7% (W = 946525, p = p < 0.001) zooplankton biomass increase compared to the nearshore baseline (Table 6). A 40% increase in PO_4 was calculated to have similar effects with phytoplankton biomass rising by 7.4% (W = 968770, p = p < 0.001) (Table 5) and a zooplankton biomass increase of 36.9% (W = 942428, p = p < 0.001) (table 6). For both DIN and PO_4 response curves, the effects of an increase associated with mussel aquaculture on phytoplankton biomass was strongest in spring (Figure 4g,h), whereas zooplankton biomass was affected most in summer (Figure 4j,k). Finally, a 50% increase in SiO_4 did not significantly affect phytoplankton, nor zooplankton biomass (Table 5, Table 6).

Table 5: *median phytoplankton biomass (overall and seasonal) for the nearshore baseline scenario as well as the responses to changes in single variables according to a mussel aquaculture scenario.*

	phytoplankton (mg Chla m^{-3}) **change compared to baseline** (%)								
	nearshore baseline	**DIN** +200%		**PO_4** +40%		**SiO_4** +50%		**Kd** +50%	
overall	**7.568**	8.119	+7.3%*	8.131	+7.4%*	7.759	+2.5%	3.457	-54.3%*
spring	**15.441**	15.859	+2.7%	15.824	+2.5%	15.632	+1.2%	6.074	-60.7%*
summer	**8.094**	8.537	+5.5%*	8.496	+5.0%*	8.160	+0.8%*	4.113	-49.2%*
fall	**6.230**	6.153	-1.2%*	6.242	+0.2%*	6.235	+0.1%	2.661	-57.3%*
winter	**4.572**	4.677	+2.3%*	4.680	+2.4%*	4.596	+0.5%	3.108	-32.0%*

** Wilcoxon rank rum test p < 0.05*

Table 6: *median zooplankton biomass (overall and seasonal) for the nearshore baseline scenario as well as the responses to changes in single variables according to a mussel aquaculture scenario.*

	zooplankton (mmol N m^{-3}) **change compared to baseline** (%)								
	nearshore baseline	**DIN** +200%		**PO_4** +40%		**SiO_4** +50%		**Kd** +50%	
overall	**0.097**	0.128	+31.7%*	0.133	+36.9%*	0.111	+13.9%	0.038	-60.8%*
spring	**0.074**	0.165	+124.4%*	0.168	+128.2%*	0.086	+16.0%	0.049	-33.7%*
summer	**0.162**	0.181	+11.8%*	0.183	+13.2%*	0.167	+3.3%*	0.059	-63.5%*
fall	**0.119**	0.131	+10.1%*	0.133	+11.9%*	0.125	+4.7%	0.045	-62.1%*
winter	**0.004**	0.005	+7.3%*	0.005	+11.34%*	0.004	-1.6%	0.004	-10.3%*

** Wilcoxon rank rum test p < 0.05*

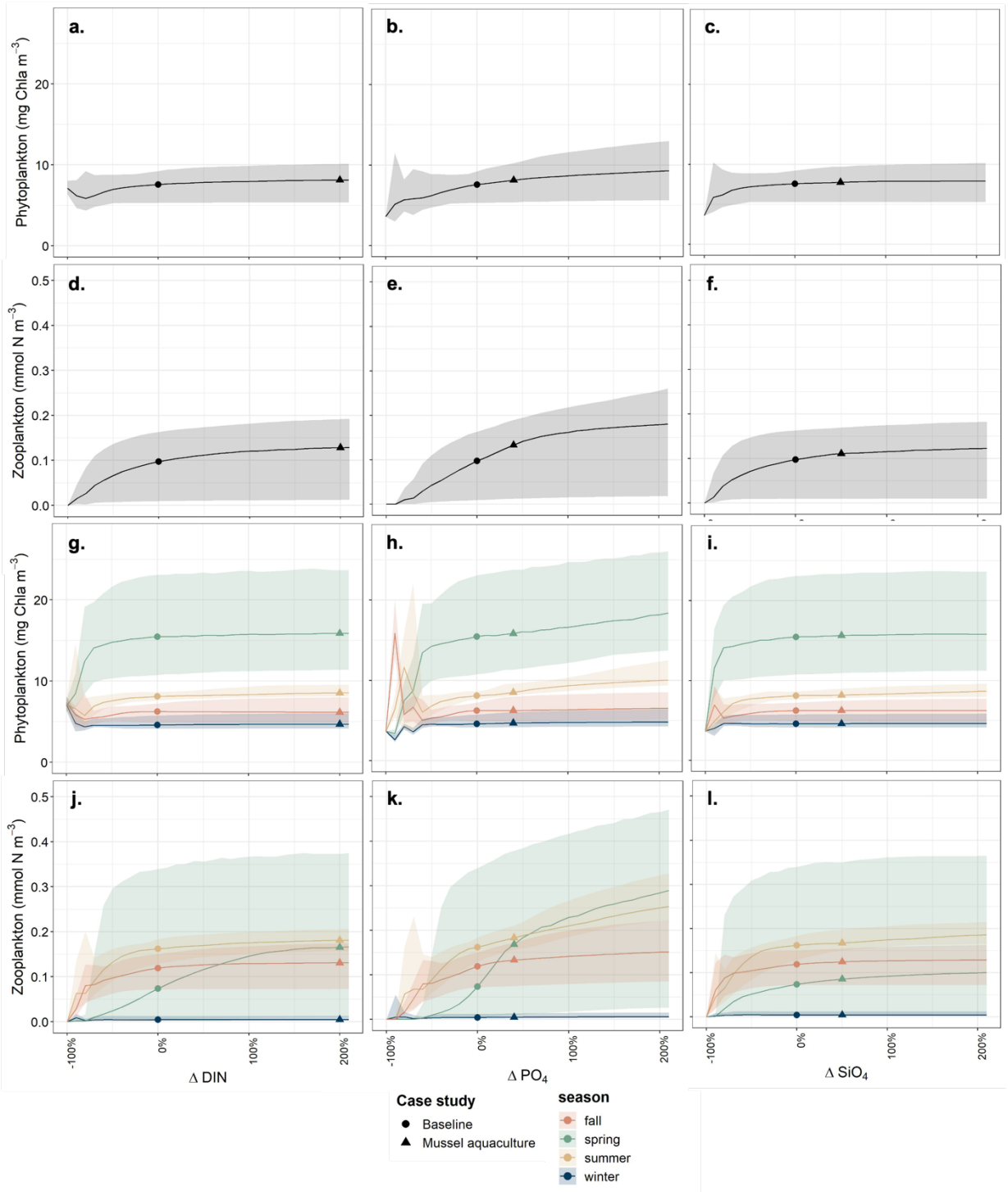

Figure 4: *Response of phytoplankton (a, b, c, g, h, i) and zooplankton (d, e, f, j, k l) biomass to changes in the concentration of a single nutrient (left to right: DIN, PO_4 and SiO_4). Gray curves represent median overall phyto- or zooplankton biomass, whereas colored curves represent seasonal median biomass. For each curve the interquartile range is marked as well. The biomass where nutrient concentrations are at nearshore baseline values is marked with a dot and a triangle marks the maximal nutrient increase associated with mussel aquaculture.*

In response to increasing changing grazing rates, a decrease in phytoplankton and zooplankton biomass was predicted (Figure 5). Throughout all simulations, spring remained the season with maximal phytoplankton biomass (Figure 5b) and summer remained the season with maximal zooplankton biomass (Figure 5d). Note that an 85% grazing increase, as well as a 10% decrease caused the model to collapse (Figure 5). For grazing rates associated with mussel aquaculture a 54.3% ($W = 1832389$, $p < 0.001$) decline in phytoplankton biomass was predicted compared to the nearshore baseline scenario, with the greatest effect observed in spring with a decline of 60.7% ($W = 127642$, $p < 0.001$) (Table 5). Overall zooplankton biomass decreased by 60.8% ($W = 133356$, $p < 0.001$) with a maximal decrease in summer with 63.5% ($W = 120126$, $p < 0.001$) (Table 6).

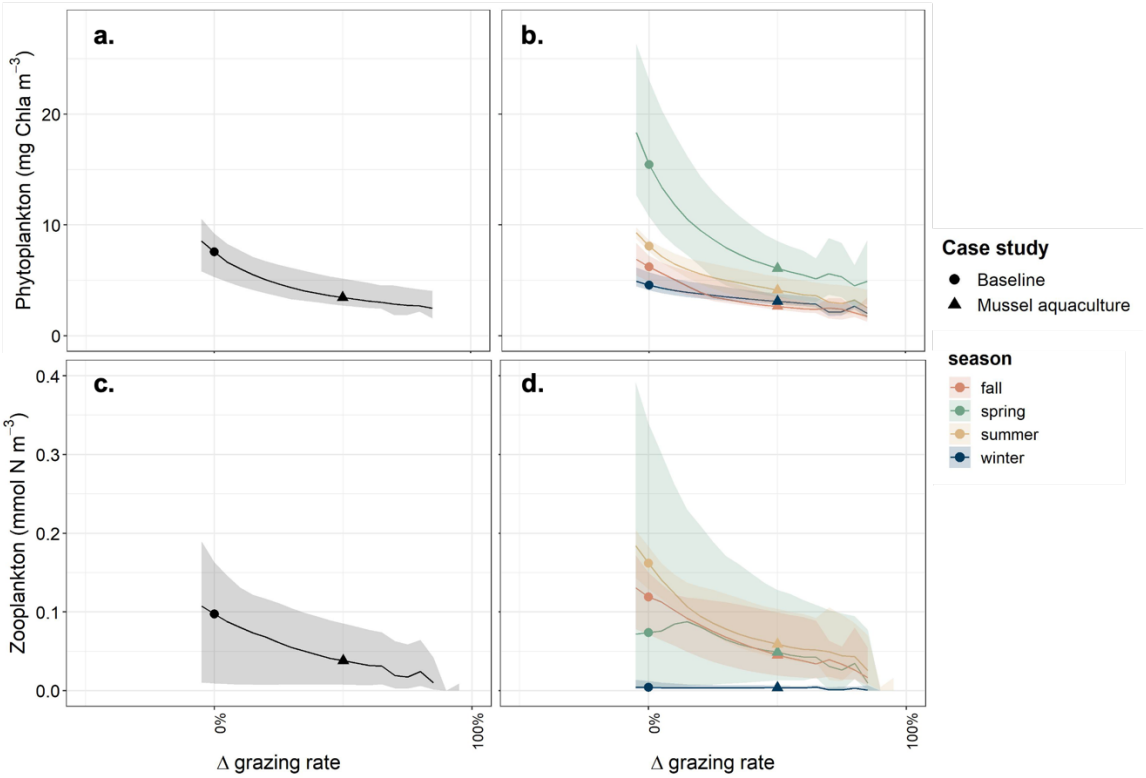

Figure 5: *Response of phytoplankton (a, b) and zooplankton (c, d) biomass to changes in grazing rate. Gray curves represent median biomass overall, whereas colored curves represent seasonal median biomass. For each curve the interquartile range is marked as well. The biomass where the grazing rate is at nearshore baseline values is marked with a dot and a triangle marks the grazing rate increase associated with mussel aquaculture.*

3.1.2 Mussel aquaculture scenario

Plankton biomass dynamics in the nearshore region of the BPNS were simulated for a baseline as well as a mussel aquaculture scenario, where nutrient availability and grazing rates were adjusted in the model accordingly. Based on simulations from 2015-2017, the introduction of mussel aquaculture in the BPNS would cause severe phyto- and zooplankton depletion. In baseline circumstances, plankton dynamics followed a clear seasonal pattern in the nearshore region. As depicted in Figure 6a, phytoplankton

biomass ranged from 3.23 to 14.75 mg Chla m^{-3}, with a spring and fall phytoplankton bloom. The maximal yearly biomass was reached during the spring bloom in May and the lowest biomass was in December. Both phytoplankton blooms were followed by a zooplankton bloom, with an approximately delay of one month. Maximal zooplankton biomass (0.20 mmol N m^{-3}) could be observed in June, whereas the minimum ($1.26*10^{-4}$ mmol N m^{-3}) was in March, right before the start of the phytoplankton spring bloom.

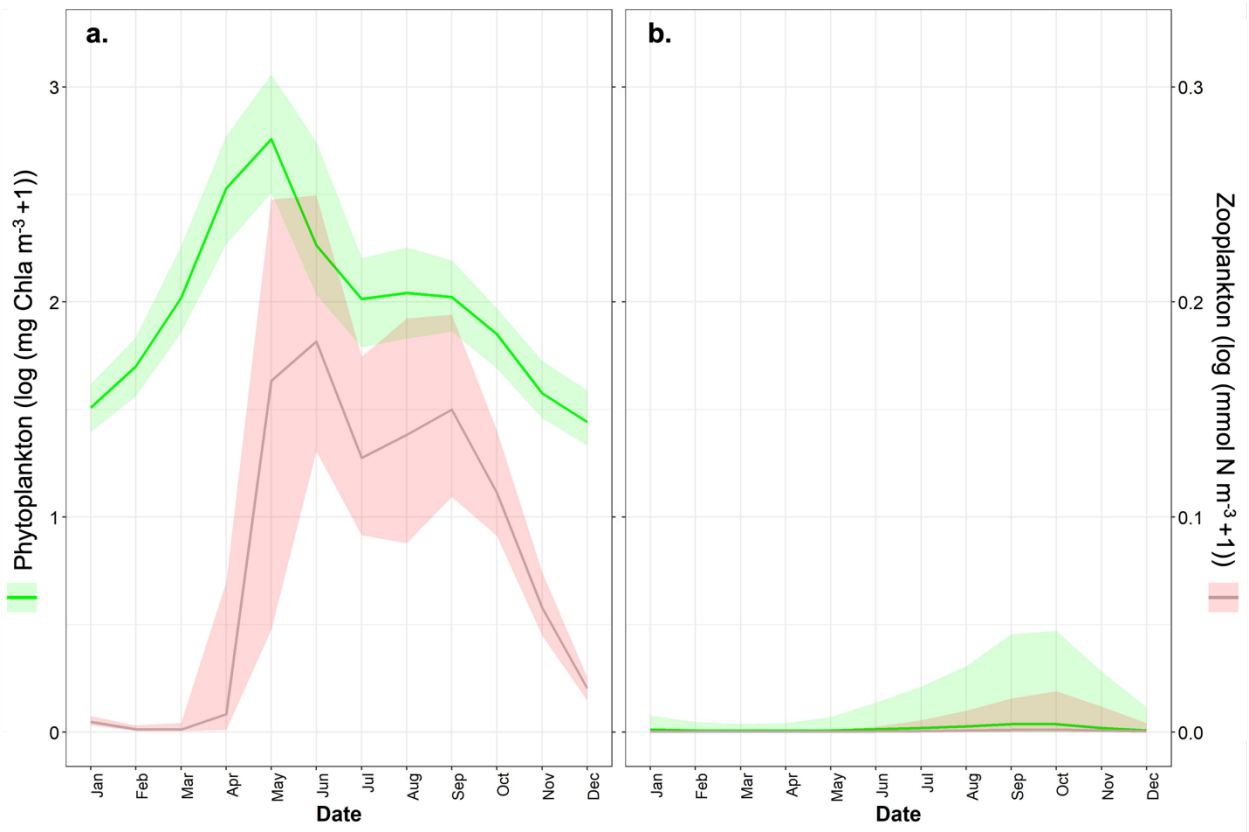

Figure 6: *Phyto- and zooplankton biomass dynamics in the nearshore baseline (a) and mussel aquaculture (b) scenario. The curves represent median phytoplankton (red) and zooplankton (green) biomass simulations from 2015-2017 and their respective interquartile ranges on a logarithmic scale.*

Compared to the baseline scenario, the integration of mussel aquaculture induced a total shift of plankton dynamics (Figure 6b). In this scenario, phytoplankton biomass ranged from 5.61E-3 Chla m^{-3} to 0.038 Chla m^{-3}. The phytoplankton maximum shifted from May towards September and was 99.7% ($W = 23$, $p < 0.001$) lower compared to the phytoplankton peak in the baseline scenario. Similar drastic phytoplankton declines were predicted in all seasons (Table 7). Alongside this phytoplankton depletion, zooplankton biomass ranged from $9.23*10^{-5}$ to $1.16*10^{-3}$ mmol N m^{-3} in March and October, respectively. Maximal zooplankton biomass decreased by 99.4% ($W = 23958$, $p < 0.001$) compared to the peak in the baseline scenario. As for phytoplankton, zooplankton depletion was predicted to persist throughout the year (Table 7).

Table 7: *Median phyto- and zooplankton biomass (overall and seasonal) for the nearshore baseline and mussel aquaculture scenario.*

	phytoplankton (mg Chla m^{-3})			zooplankton (mmol N m^{-3})		
	nearshore baseline	**mussel aquaculture**	**change**	**nearshore baseline**	**mussel aquaculture**	**change**
overall	5.801	0.012	-99.8%*	0.065	$2.56*10^{-04}$	-99.6%*
peak	14.749	0.038	-99.7%*	0.20	$1.16*10^{-03}$	-99.4%*
spring	10.284	$6.30*10^{-03}$	-99.9%*	8.71E-03	$1.04*10^{-04}$	-98.8%*
summer	7.107	0.018	-99.8%*	0.159	$4.00*10^{-04}$	-99.8%*
fall	5.017	0.031	-99.4%*	0.104	$9.62*10^{-04}$	-99.1%*
winter	3.695	0.009	-99.8%*	0.006	$2.07*10^{-04}$	-96.5%*

** Wilcoxon rank rum test p < 0.05*

3.2 Offshore wind farm

3.2.1 Response curves

To explore the effect of suspended particulate matter plumes caused by offshore wind infrastructure, the phyto- and zooplankton biomass responses to changes in turbidity were calculated using the NPZD model. For changes in Kd ranging from -100% to +80%, no clear positive or negative trend in overall phytoplankton biomass was predicted by the model. However, within this range the seasonal dynamics were continuously shifting (Figure 7b). For zooplankton biomass a negative trend was predicted in relation to increasing turbidity, with a continuously shifting seasonality as well. Note that this trend was especially prominent at low Kd values beneath a 40% decline. At a 70% Kd increase, zooplankton was predicted to be almost completely depleted with the biomass never again reaching $1.11*10^{-12}$ mmol N m^{-3}. Following this lack of zooplankton, from a Kd increase of 75% onwards the phytoplankton biomass starts to decrease down to a minimum of 0.935 mg Chl m^{-3}. Compared to the offshore baseline scenario, a Kd increase of 43% associated with offshore wind infrastructure was predicted to decrease overall phytoplankton biomass by 9.1% ($W = 1181637$, $p < 0.001$) (Table 8), though there was no significant change in overall zooplankton biomass (Table 9). However, in fall and winter the model simulated a decrease in zooplankton biomass of 64.5% ($W = 80527$, $p < 0.001$) and 39.1% ($W = 74572$, $p < 0.001$), respectively (Table 9).

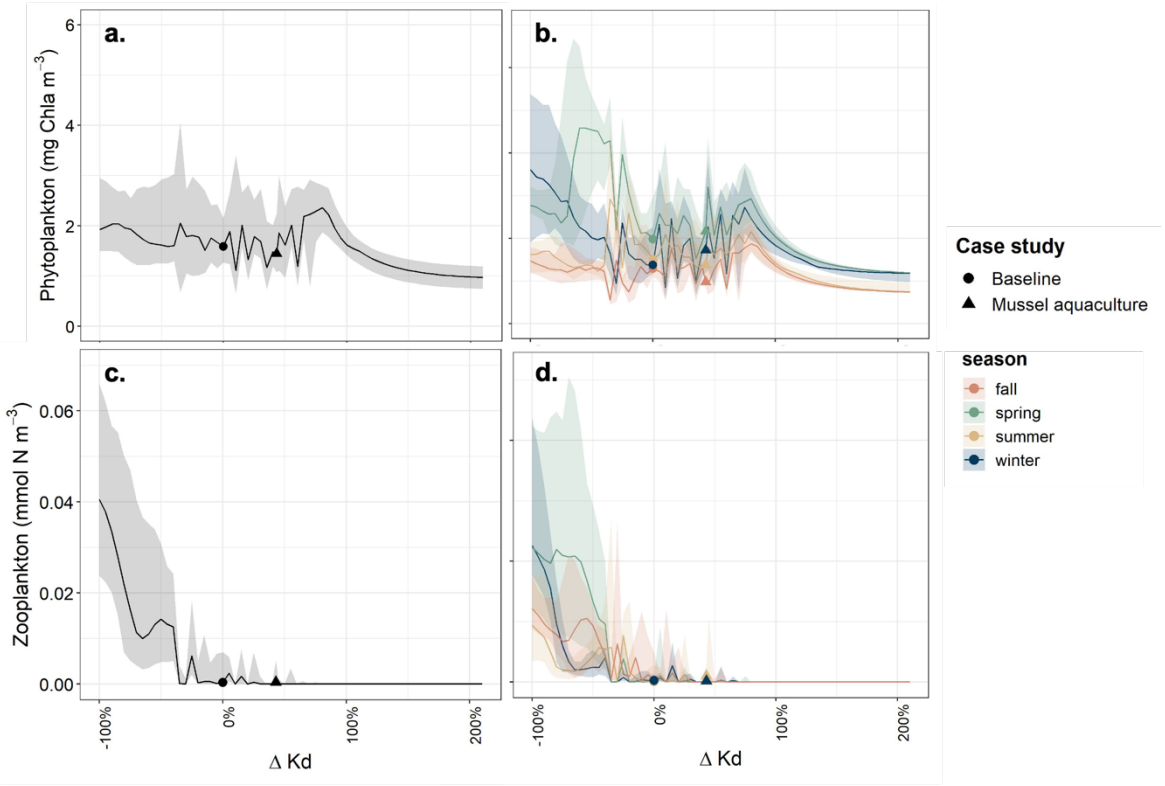

Figure 7: *Response of the overall (top) and seasonal (bottom) phytoplankton and zooplankton biomass to changes in Kd. Solid lines represent the overall (left) and seasonal (right) median biomass, whereas the shaded ribbons represent the interquartile range. Solid lines represent the overall (left) and seasonal (right) median biomass, whereas the shaded ribbons represent the interquartile range. A dot and a triangle mark the phyto- or zooplankton biomass in the offshore baseline scenario and the offshore wind scenario respectively.*

Table 8: *Median phytoplankton biomass (overall and seasonal) for the offshore baseline scenario as well as the response to changes in Kd associated with an offshore wind scenario.*

phytoplankton (mg Chla m^{-3}) **change compared to baseline** (%)			
	offshore baseline	**Kd** +50%	
overall	1.589	1.445	-9.0%*
spring	1.982	2.165	9.2%
summer	1.505	1.374	-8.7%*
fall	1.292	0.978	-24.3%*
winter	1.379	1.726	25.1%

** Wilcoxon rank rum test $p < 0.05$*

Table 9: *Median zooplankton biomass (overall and seasonal) for the offshore baseline scenario as well as the response to changes in Kd associated with an offshore wind scenario.*

zooplankton biomass (mmol N m^{-3}) **change compared to baseline** (%)			
	offshore baseline	**Kd** +50%	
overall	$3.21*10^{-04}$	$4.04*10^{-04}$	25.9%
spring	$1.71*10^{-04}$	$4.98*10^{-04}$	190.8%
summer	$1.87*10^{-04}$	$2.50*10^{-03}$	1235.8%
fall	$8.79*10^{-04}$	$3.12*10^{-04}$	-64.5%*
winter	$6.69*10^{-04}$	$4.08*10^{-04}$	-39.1%*

** Wilcoxon rank rum test p < 0.05*

3.2.2 Offshore wind farm scenario

Plankton biomass dynamics were simulated for the offshore region in a baseline and offshore wind farm scenario. When simulations from 2015-2017 were compared, shifts in both phyto- and zooplankton dynamics were observed. In the offshore region, baseline phytoplankton dynamics were characterized by a large spring bloom, and a smaller summer and fall bloom (Figure 7a). Phytoplankton biomass ranged from 2.15 to 6.51 mg Chla m^{-3} throughout the year, with maximal biomass in February during the early spring bloom and a minimum in September. Zooplankton biomass followed this three-bloom pattern as well with a minimum biomass in June (0.017 mmol N m^{-3}) and a maximum biomass (0.14 mmol N m^{-3}) in March.

The introduction of offshore wind infrastructure into the model resulted in a shift in the plankton bloom pattern from three yearly blooms towards two (Figure 7b). Throughout this pattern phytoplankton biomass ranged from 3.25 to 9.27 mg Chla m^{-3}. The phytoplankton biomass maximum in this scenario was predicted to be in June and increased by 42.5% compared to the nearshore baseline ($W = 7134528$, $p < 0.001$) (Table 10). The median phytoplankton biomass throughout the year increased as well by 50.5% ($W = 1096259904$, $p < 0.001$). In fact, increased phytoplankton biomass was predicted in all seasons except winter, where a 14.8% decline was calculated ($W = 37220153$, $p < 0.001$) (Table 10). Associated with the shift of the yearly phytoplankton biomass peak from February towards June, the greatest seasonal phytoplankton biomass change was seen in summer with a 231.9% increase ($W = 92251210$, $p < 0.01$). Contrary to phytoplankton, overall zooplankton biomass declined by 95.3% in the offshore wind scenario ($W = 344648495$, $p < 0.001$) and ranged from $3.94*10^{-5}$ to 0.041 mmol N m^{-3}. The zooplankton peak biomass decreased by 71.2% ($W = 3109515$, $p < 0.001$) and a zooplankton decline was predicted in all seasons with the largest differences observed in spring and summer (Table 10).

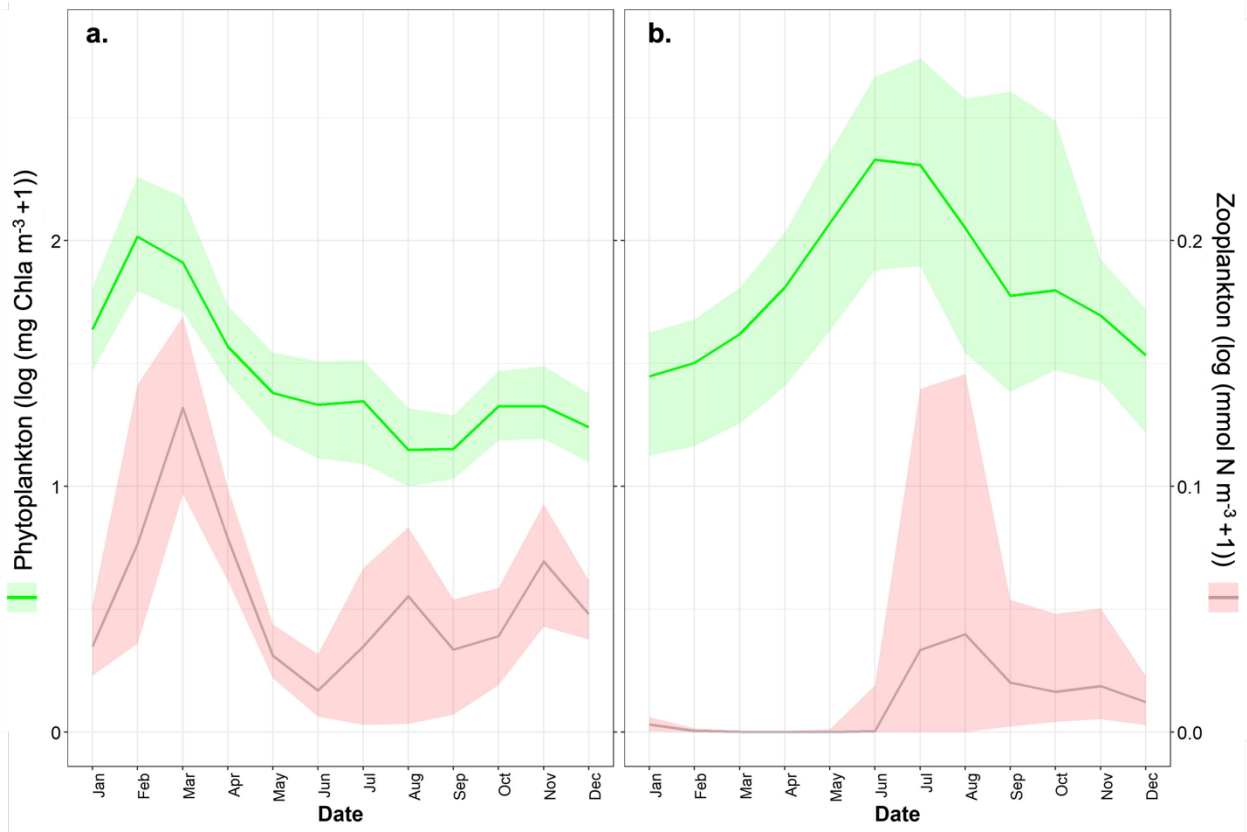

Figure 8: *Phyto- and zooplankton biomass dynamics in the offshore baseline (a) and offshore wind (b) scenario. The curves represent median phytoplankton (red) and zooplankton (green) biomass simulations from 2015-2017 and their respective interquartile ranges on a logarithmic scale.*

Table 10: *median phyto- and zooplankton biomass (overall and seasonal) for the offshore baseline and offshore wind scenario.*

	phytoplankton (mg Chla m^{-3})			**zooplankton** (mmol N m^{-3})		
	offshore baseline	**offshore wind**	**change**	**offshore baseline**	**offshore wind**	**change**
overall	3.092	4.653	+50.5%*	0.049	$2.29*10^{-03}$	-95.3%*
peak	6.507	9.273	+42.5%*	0.141	0.041	-71.2%*
spring	3.932	4.924	+25.2%*	0.075	$5.91*10^{-05}$	-99.9%*
summer	2.541	8.433	+231.9%*	0.028	0.011	-60.0%*
fall	2.571	4.716	+83.4%*	0.046	0.018	-59.9%*
winter	4.049	3.450	-14.8%*	0.049	$2.41*10^{-03}$	-95.1%*

** Wilcoxon rank rum test $p < 0.05$*

4. Discussion

An NPZD model was used to quantify the effects of potential blue economy developments on plankton biomass dynamics in the BPNS. Specifically, the impact of mussel aquaculture and offshore wind farms were investigated, two commercial activities for which the effect on phyto- and zooplankton biomass had not yet been fully explored in the BPNS.

4.1 Mussel aquaculture

To assess the impact of mussel aquaculture on plankton biomass dynamics, this thesis study focused on how this commercial activity alters nutrient concentrations and phytoplankton grazing rates. Both changes were found to affect phyto- and zooplankton biomass significantly. Alterations in separate nutrient concentrations (DIN, PO_4, SiO_4) as well as in all nutrients simultaneously were investigated. All of the resulting plankton biomass response curves indicated a positive relationship between nutrient availability and plankton biomass (Figure 3, Figure 4). A simultaneous concentration increase in all nutrients of 90% led to model collapse, whereas separate response curves rose to a phyto- and zooplankton biomass limit in a manner that approaches logarithmic growth curves. This maximum is likely reached when phyto- and zooplankton biomass are no longer limited by the concentration of the nutrient of interest. The stronger plankton biomass response to changes in all nutrients compared to changes in single nutrients (Figure 3, Figure 4), can be explained by nutrient co-limitation (Harpole et al., 2011). In addition, previous studies have shown that when nutrient availability is high, competition for light becomes increasingly important (Burkholder & Glibert, 2013). Laboratory experiments by Burson et al. (2018), for example, found that increasing nutrient loads change phytoplankton species composition due to a shift from interspecies competition for competition for light. Response curves for zooplankton biomass were similarly shaped to those for phytoplankton biomass. This suggests food availability (i.e., phytoplankton) to be the main limiting factor for zooplankton growth in the BPNS. Notably, previous studies have shown phyto- and zooplankton biomass can also respond in opposite manners to environmental changes. For example, in the Bohai Sea a decrease in zooplankton has been observed alongside increased phytoplankton biomass related to ocean acidification and warming (Wei et al., 2022). The absence of such an effect could be due to either local conditions in the BPNS, or the nature of the NPZD model. For example, oxygen levels were not incorporated in the model calculations whilst deoxygenation is often associated with eutrophication and can negatively impact zooplankton growth (Wishner et al., 2018). By projecting the specific changes in nutrient concentrations associated with mussel aquaculture (Table 2) onto the response curves, it became clear that both the expected DIN and PO_4 increases would significantly affect phyto- and zooplankton biomass throughout the year (Table 5, Table 6). Whereas the expected increase in SiO_4 did not significantly affect either overall phyto- or zooplankton biomass. Note that the strongest overall phytoplankton (+7.4%) (Table 5) and zooplankton (+36.9%) (Table 6) biomass increases were predicted for PO_4. This is in accordance with results from Burson et al. (2016) who determined phosphorus to be the most limiting nutrient in the coastal waters of the Southern Bright of the North Sea. Bear in mind that in these response curves the seasonality of changes in nutrient concentration due to mussel aquaculture was not incorporated. This could cause the predicted plankton biomass response to be magnified.

Next, the response of plankton biomass to changes in phytoplankton grazing was investigated, and a negative relationship was found between plankton biomass and grazing rates (Figure 5). A small grazing decline of 10% resulted in a model collapse due to phytoplankton concentrations reaching the realistic maximal value allowed by the NPZD model. This suggests a strong top-down grazing control of phytoplankton biomass at baseline circumstances, although the relative importance of top-down and bottom-up controls in marine ecosystems remains contested (Hunt & McKinnell, 2006). At rising grazing rates, the model collapses at an 85% grazing increase, because the realistic minimal phytoplankton biomass allowed by the model is reached. When grazing rates associated with mussel aquaculture were projected onto the response curves, an overall 54.3% decline in phytoplankton (Table 5) and a 60.8% decline in zooplankton biomass (Table 6) were predicted. This is in accordance with previous findings that reported bivalve grazing to induce top-down control on phytoplankton biomass and community composition (Prins et al., 1998). Note that the dependence of mussel grazing on phytoplankton biomass due to valve closure was not incorporated in these response curve calculations.

Finally, to quantify the effect of mussel aquaculture on plankton biomass dynamics, both changes in nutrient concentrations (including seasonal dynamics) and mussel grazing (including dependence on chlorophyll concentration) were incorporated in the model. The simulations indicate that the introduction of mussel aquaculture in the nearshore region of the BPNS would cause severe phyto- and zooplankton depletion with seasonal biomass declines ranging from 96.4% to 99.9% (Table 7). In comparison, reported phytoplankton depletion in the presence of commercial mussel aquaculture ranges from no depletion at all to a 30% phytoplankton concentration decrease (Cranford et al., 2008; Ogilvie, 2000; Petersen et al., 2008). The extreme depletion predicted in this thesis, was calculated based on a closed ecosystem model, which can result in exaggerated effects of a changing environment on plankton biomass dynamics. Previously reported changes in phytoplankton biomass associated with mussel aquaculture vary strongly based on local conditions. In certain areas, such as Beatrix Bay in New Zealand, a phytoplankton concentration increase has been reported in winter instead of depletion (Ogilvie et al., 2000). In these instances, the bottom-up phytoplankton biomass driver of mussel nutrient regeneration may have outweighed the top-down control of mussel grazing (Prins et al., 1998). This highlights the spatiotemporal variability associated with plankton dynamics and their responses to environmental changes (Heinle et al., 2021; Yebra et al., 2022).

4.2 Offshore wind farm

Offshore wind farms are associated with suspended particulate matter (SPM) blooms and thus increased turbidity, which could affect plankton dynamics (Forster, 2018; Vanhellemont & Ruddick, 2014). This was confirmed by the Kd response curves calculated in this thesis, based on the NPZD model. At low turbidity levels (< Kd -40%) phytoplankton biomass remains constant, whereas zooplankton biomass shows a strong positive relationship with increasing light availability (Figure 7). This suggests that when light would not be a limiting factor in the BPNS, top-down control by zooplankton grazing could become increasingly important. At high turbidity levels (> Kd +70%) on the other hand, phytoplankton biomass starts decreasing whilst zooplankton biomass is almost completely depleted (Figure 7). In this case, phytoplankton biomass appears to be mainly bottom-up controlled. In general, the relative importance

of bottom-up and top-down controls has been shown to be highly variable in marine ecosystems related to local environmental conditions (Hunt & McKinnell, 2006; Lindegren et al., 2018; Litzow & Ciannelli, 2007). Whenever the change in turbidity remains within a range of Kd -40% and +70% an unstable balance between bottom-up and top-down control results in continuously shifting seasonality in both phyto- and zooplankton biomass (Figure 7). When the estimated turbidity increase associated with SPM plumes (Kd +43%) was projected onto these response curves, an overall decrease in phytoplankton biomass of 9.1% was predicted (Table 8). Overall zooplankton biomass did not increase significantly when turbidity levels reflected those for offshore wind farms, although a seasonal decrease was predicted in both fall (-64.5%) and winter (-39.1%) (Table 9). This was likely in response to the seasonal declines of phytoplankton in summer (-8.7%) and fall (-24.2%) (Table 8), since zooplankton blooms usually follow phytoplankton blooms with some time lag (Almén & Tamelander, 2020).

Finally, the NPZD model was used to simulate the presence of a wind farm in the offshore region of the BPNS, resulting in a shift in seasonal plankton biomass dynamics. The simulations indicated a wind farm in the offshore region of the BPNS would increase overall phytoplankton biomass by 50.5% and decrease overall zooplankton biomass by 95.3% (Table 10). Similar biomass shifts were observed throughout all seasons. As stated previously, opposite phyto- and zooplankton biomass responses to changes in the marine environment have been recorded before in the Bohai Sea (Wei et al., 2022). However, these predicted phyto- and zooplankton dynamics differ strongly compared to the results of the Kd response curves. These curves suggested that a 43% Kd increase would cause a decrease in overall phytoplankton biomass and an unchanged zooplankton biomass. This disparity is likely due to the methodological differences between the response curve calculations and the plankton dynamics simulations. In essence, the response curves were based on a single model iteration, whereas for the plankton dynamics 5000 iterations were run. In addition to the introduction of increased model variation, the 43% Kd increase also falls within the section of the response curve where there was an unstable balance between top-down and bottom-up control either way. Most previous studies observed phytoplankton biomass declines associated with decreased light availability (Alpine & Cloern, 1988; Marzetz et al., 2020). In estuaries for example, a primary productivity gradient can be observed following the turbidity gradient of a river plume (Cloern, 1987). In addition to biomass changes in both phyto- and zooplankton, the seasonal pattern in the offshore region of the BPNS shifted from three seasonal blooms towards two according to model predictions (Figure 8). During the past four decades, phytoplankton seasonality shifts have been observed in the BPNS associated with changes in nutrient concentrations, turbidity, and SST (Nohe et al., 2020). Notably, the predicted plankton dynamics for an offshore wind farm look similar to nearshore baseline dynamics. In this region there are also two seasonal phytoplankton blooms, although the timing is slightly different compared to the offshore wind farm scenario. This might be explained by the baseline turbidity in the nearshore area, which is generally higher compared to more offshore regions in the North Sea (Fettweis & Van Den Eynde, 2003).

4.3 NPZD model: advantages, limitations, and future prospects

In research on complex ecosystem interactions such as plankton dynamics, laboratory studies are often used to discern the effects of multiple environmental drivers. This has the advantage that species can be

kept in optimal conditions to isolate the effects of any stressor in question. However, it can be difficult to generalize observed effects from a laboratory setting, since in nature these optimal situations generally do not occur (Aziz, 2017). Modeling approaches based on field data can bridge this gap, allowing the implicit integration of natural variation into study results. The model calculations applied in this thesis were based on input data collected in the field (i.e. SST, nutrients, and solar irradiance), although for the two hypothetical scenarios, currently no *in situ* plankton biomass data is available to validate model findings. Additionally, since the model adjustments associated with mussel aquaculture and offshore wind farms were based on data from different study areas, it cannot be guaranteed that the same activities in the BPNS would have similar environmental effects. It is also important to note that the NPZD model is a closed ecosystem model. This could result in exaggerated plankton biomass changes in response to altered environmental conditions. Alternatively, spatially explicit models allow the inclusion of hydrodynamics, which may be an important driver of plankton dynamics. Such a model has been developed previously by Grant et al. (2008), for example, to investigate how mussel aquaculture in Tracady Bay (Canada) affects phytoplankton concentration. Extending the current model into a spatially explicit model could be a valuable next step to investigate the effects of commercial activities on plankton dynamics in the BPNS. Nevertheless, the modeling assessment of mussel aquaculture and offshore wind farms conducted in this thesis, indicates that both economic developments have the potential to impact phyto- and zooplankton biomass dynamics in the BPNS. This highlights the need to monitor such economic developments. Additional data collected in the field could be used to further calibrate and validate the NPZD model to accurately describe plankton dynamics in mussel aquaculture sites and offshore wind farms. The model could also be used to assess the impact of other commercial activities. This could then become a useful tool for legislators and stakeholders to improve the assessment, permitting and marine spatial planning of commercial activities in the BPNS.

5. Conclusion

In this thesis, the potential effects of mussel aquaculture and offshore wind farms on plankton dynamics in the BPNS were explored and quantified. Both commercial activities were found to affect plankton biomass, as well as seasonal bloom patterns. According to the model predictions, the introduction of mussel aquaculture in the nearshore area of the BPNS would cause severe phyto- and zooplankton depletion in all seasons. The development of a wind farm in the offshore region could alter seasonal plankton dynamics, reducing the number of yearly blooms from three to two. A modeling approach such as described in this thesis can be used to study several other economic developments, as well as climate change effects on plankton dynamics in the BPNS. This could be a useful tool for legislators and stakeholders to promote science-supported decision making, by assessing and predicting the ecological impact of economic activities and to improve marine spatial planning practices.

6. Data and script availability

Datasets and scripts related to this master thesis can be found at *https://doi.org/10.14284/603*, hosted on the Integrated Marine Information System (IMIS) from the Flanders Marine Institute (VLIZ).

7. Acknowledgements

This thesis was conducted as a collaborative effort between the Ocean & Human Health research department at the Flanders Marine Institute (VLIZ), and the Marine Biology research group at Ghent University. The work relied on LifeWatch data and infrastructure funded by Research Foundation Flanders (FWO) as part of the Belgian contribution to LifeWatch ESFRI. We would like to thank the crew from RV Simon Stevin for this data collection. Additionally, data from Monitoring Network Flemish Banks ('Meetnet Vlaamse Banken') was used, published by the Flemish government 'Agency Maritime Services and Coast' (IVA MDK).

7. References

Almén, A. K., & Tamelander, T. (2020). Temperature-related timing of the spring bloom and match between phytoplankton and zooplankton. *Marine Biology Research*, *16*(8–9), 674–682. https://doi.org/10.1080/17451000.2020.1846201

Alpine, A. E., & Cloern, J. E. (1988). Phytoplankton growth rates in a light-limited environment, San Francisco Bay. *Marine Ecology Progress Series*, *44*, 167–173. https://www.jstor.org/stable/24825726

Aziz, H. A. (2017). Comparison between Field Research and Controlled Laboratory Research. *Archives of Clinical and Biomedical Research*, *1*(2), 101–104. http://dx.doi.org/10.26502/acbr.50170011

Baeye, M., & Fettweis, M. (2015). In situ observations of suspended particulate matter plumes at an offshore wind farm, southern North Sea. *Geo-Marine Letters*, *35*, 247–255. https://doi.org/10.1007/s00367-015-0404-8

Blauw, A. N., Benincà, E., Laane, R. W. P. M., Greenwood, N., & Huisman, J. (2018). Predictability and environmental drivers of chlorophyll fluctuations vary across different time scales and regions of the North Sea. *Progress in Oceanography*, *161*, 1–18. https://doi.org/10.1016/j.pocean.2018.01.005

Burkholder, J. A. M., & Glibert, P. M. (2013). Eutrophication and Oligotrophication. In *Encyclopedia of Biodiversity: Second Edition* (pp. 347–371). Elsevier Inc. https://doi.org/10.1016/B978-0-12-384719-5.00047-2

Burson, A., Stomp, M., Akil, L., Brussaard, C. P. D., & Huisman, J. (2016). Unbalanced reduction of nutrient loads has created an offshore gradient from phosphorus to nitrogen limitation in the North Sea. *Limnology and Oceanography*, *61*(3), 869–888. https://doi.org/10.1002/lno.10257

Burson, A., Stomp, M., Greenwell, E., Grosse, J., & Huisman, J. (2018). Competition for nutrients and light: testing advances in resource competition with a natural phytoplankton community. *Ecology*, *99*(5), 1108–1118. https://doi.org/10.1002/ecy.2187

Cavan, E. L., Henson, S. A., Belcher, A., & Sanders, R. (2017). Role of zooplankton in determining the efficiency of the biological carbon pump. *Biogeosciences*, *14*(1), 177–186. https://doi.org/10.5194/bg-14-177-2017

Chassot, E., Bonhommeau, S., Dulvy, N. K., Mélin, F., Watson, R., Gascuel, D., & Le Pape, O. (2010). Global marine primary production constrains fisheries catches. *Ecology Letters*, *13*, 495–505. https://doi.org/10.1111/j.1461-0248.2010.01443.x

Cloern, J. E. (1987). Turbidity as a control on phytoplankton biomass and productivity in estuaries. *Continental Shelf* Research, 7, 1367–1381. https://doi.org/10.1016/0278-4343(87)90042-2

Cranford, P. J., Li, W., Strand, Ø., & Strohmeier, T. (2008). Phytoplankton depletion by mussel aquaculture: high resolution mapping, ecosystem modeling and potential indicators of ecological carrying capacity. In *International Council for the Exploration of the Seas; Theme H: Ecological Carrying Capacity in Shellfish Aquaculture*. https://doi.org/10.1016/j.aquaculture.2023.739659

Cugier, P., Struski, C., Blanchard, M., Mazurié, J., Pouvreau, S., Olivier, F., Trigui, J. R., & Thiébaut, E. (2010). Assessing the role of benthic filter feeders on phytoplankton production in a shellfish farming site: Mont Saint Michel Bay, France. *Journal of Marine Systems*, *82*, 21–34. https://doi.org/10.1016/j.jmarsys.2010.02.013

Dauwe, S., Verleye, T., Pirlet, H., Martens, C., Sandra, M., De Raedemaecker, F., Devriese, L., Lescrauwaet, A., Depoorter, M., & Mees, J. (2022). *Knowledge Guide Coast and Sea 2022 - Compendium for Coast and Sea*. https://doi.org/10.48470/25

Davenport, E. D., Fan, C., Govoni, J. J., & Anderson, J. (2012). Description and Application of a NPZD Model to Forecast Hurricane Impacts to Secondary Production in Coastal Ecosystems. *Procedia Environmental Sciences*, *13*, 1569–1584. https://doi.org/10.1016/j.proenv.2012.01.149

De Baar, H. J. W. (1994). Von Liebig's law of the minimum and plankton ecology (1899-1991). *Progress in Oceanography*, *33*, 347–386. https://doi.org/10.1016/0079-6611(94)90022-1

Degraer, S., Brabant, R., Rumes, B., & Vigin, L. (2020a). *Environmental impacts of offshore wind farms in the Belgian part of the North Sea: empirical evidence inspiring priority monitoring, research and management*. www.naturalsciences.be

Degraer, S., Carey, D. A., Coolen, J. W. P., Hutchison, Z. L., Kerckhof, F., Rumes, B., & Vanaverbeke, J. (2020b). Offshore wind farm artificial reefs affect ecosystem structure and functioning: a synthesis. *Oceanography*, *33*(4), 48–57. https://doi.org/10.5670/oceanog.2020.405

Devlin, M. J., Barry, J., Mills, D. K., Gowen, R. J., Foden, J., Sivyer, D., & Tett, P. (2008). Relationships between suspended particulate material, light attenuation and Secchi depth in UK marine waters. *Estuarine, Coastal and Shelf Science*, *79*(3), 429–439. https://doi.org/10.1016/j.ecss.2008.04.024

Doney, S. C., Ruckelshaus, M., Duffy, E. J., Barry, J. P., Chan, F., English, C. A., Galindo, H. M., Grebmeier, J. M., Hollowed, A. B., Knowlton, N., Polovina, J., Rabalais, N. N., Sydeman, W. J., & Talley, L. D. (2012). Climate change impacts on marine ecosystems. *Annual Review of Marine Science*, *4*, 11–37. https://doi.org/10.1146/annurev-marine-041911-111611

Everaert, G., De Laender, F., Goethals, P. L. M., & Janssen, C. R. (2015). Relative contribution of persistent organic pollutants to marine phytoplankton biomass dynamics in the North Sea and the Kattegat. *Chemosphere*, *134*, 76–83. https://doi.org/10.1016/j.chemosphere.2015.03.084

Fettweis, M., & Van Den Eynde, D. (2003). The mud deposits and the high turbidity in the Belgian-Dutch coastal zone, southern bight of the North Sea. *Continental Shelf Research*, *23*(7), 669–691. https://doi.org/10.1016/S0278-4343(03)00027-X

Field, C. B., Behrenfeld, M. J., Randerson, J. T., & Falkowski, P. (1998). Primary Production of the Biosphere: Integrating Terrestrial and Oceanic Components. *Science*, *281*, 237–240. https://doi.org/10.1126/science.281.5374.237

Floeter, J., van Beusekom, J. E. E., Auch, D., Callies, U., Carpenter, J., Dudeck, T., Eberle, S., Eckhardt, A., Gloe, D., Hänselmann, K., Hufnagl, M., Janßen, S., Lenhart, H., Möller, K. O., North, R. P., Pohlmann, T., Riethmüller, R., Schulz, S., Spreizenbarth, S., … Möllmann, C. (2017). Pelagic effects of offshore wind farm foundations in the stratified North Sea. *Progress in Oceanography*, *156*, 154–173. https://doi.org/10.1016/j.pocean.2017.07.003

Forster, R. M. (2018). *The effect of monopile-induced turbulence on local suspended sediment pattern around UK wind farms: field survey report.* www.hull.ac.uk/iecs

González, J., Fernández, E., & Figueiras, F. G. (2022). Assessing the effect of oil spills on the dynamics of the microbial plankton community using a NPZD model. *Estuarine, Coastal and Shelf Science*, *265*. https://doi.org/10.1016/j.ecss.2021.107734

Grant, J., Bacher, C., Cranford, P. J., Guyondet, T., & Carreau, M. (2008). A spatially explicit ecosystem model of seston depletion in dense mussel culture. *Journal of Marine Systems*, *73*(1–2), 155–168. https://doi.org/10.1016/j.jmarsys.2007.10.007

Halpern, B. S., Selkoe, K. A., Micheli, F., & Kappel, C. V. (2007). Evaluating and ranking the vulnerability of global marine ecosystems to anthropogenic threats. *Conservation Biology*, *21*(5), 1301–1315. https://doi.org/10.1111/j.1523-1739.2007.00752.x

Harpole, W. S., Ngai, J. T., Cleland, E. E., Seabloom, E. W., Borer, E. T., Bracken, M. E. S., Elser, J. J., Gruner, D. S., Hillebrand, H., Shurin, J. B., & Smith, J. E. (2011). Nutrient co-limitation of primary producer communities. *Ecology Letters*, *14*, 852–862. https://doi.org/10.1111/j.1461-0248.2011.01651.x

Heinle, M. J., Kolchar, R. M., Flandez, A. V., Clardy, T. R., Thomas, B. K., Hikmawan, T. I., Prihartato, P. K., Abdulkader, K. A., & Qurban, M. A. (2021). Spatial and temporal variability in the phytoplankton community of the Western Arabian Gulf and its regulation by physicochemical factors and zooplankton. *Regional Studies in Marine Science*, *47*. https://doi.org/10.1016/j.rsma.2021.101982

Heneghan, R. F., Everett, J. D., Blanchard, J. L., Sykes, P., & Richardson, A. J. (2023). Climate-driven zooplankton shifts cause large-scale declines in food quality for fish. *Nature Climate Change*. https://doi.org/10.1038/s41558-023-01630-7

Hunt, G. L., & McKinnell, S. (2006). Interplay between top-down, bottom-up, and wasp-waist control in marine ecosystems. *Progress in Oceanography*, *68*, 115–124. https://doi.org/10.1016/j.pocean.2006.02.008

IPCC. (2021). *Climate Change 2021: The Physical Science Basis. Contribution of Working Group I to the Sixth Assessment Report of the Intergovernmental Panel on Climate Change* (V. Masson-Delmotte, P. Zhai, A. Pirani, S. L. Connors, C. Péan, S. Berger, C. Naud, Y. Chen, L. Goldfarb, M. I. Gomis, M. Huang, K. Leitzell, E. Lonnoy, J. B. R. Matthews, T. K. Maucock, T. Waterfield, O. Yelekçi, R. Yu, & B. Zhou, Eds.). Cambridge University Press. https://doi.org/10.1017/9781009157896

Irigoien, X., Flynn, K. J., & Harris, R. P. (2005). Phytoplankton blooms: A “loophole” in microzooplankton grazing impact? *Journal of Plankton Research*, *27*(4), 313–321. https://doi.org/10.1093/plankt/fbi011

IVA MDK. (n.d.). *Monitoring Network Flemish Banks [Meetnet Vlaamse Banken]*.

Jacobs, P. (2015). *The impact of pelagic mussel collectors on plankton in the western Wadden Sea, the Netherlands*.

Käse, L., & Geuer, J. K. (2018). Phytoplankton Responses to Marine Climate Change – An Introduction. In *YOUMARES 8 – Oceans Across Boundaries: Learning from each other* (pp. 55–71). Springer International Publishing. https://doi.org/10.1007/978-3-319-93284-2_5

Kirk, J. T. O. (1994). *Light and Photosynthesis in Aquatic Ecosystems* (2nd ed.). Cambridge University Press, New York.

Lacroix, G., Ruddick, K., Gypens, N., & Lancelot, C. (2007). Modelling the relative impact of rivers (Scheldt/Rhine/Seine) and Western Channel waters on the nutrient and diatoms/Phaeocystis distributions in Belgian waters (Southern North Sea). *Continental Shelf Research*, *27*, 1422–1446. https://doi.org/10.1016/j.csr.2007.01.013

Lagring, R., Bekaert, K., Borges, A. V., De Witte, B., Desmit, X., Minh Le, H., Nohe, A., Sabbe, K., Strobbe, F., Tyberghein, L., Vandenberghe, T., & Van Der Zande, D. (2018). *4 Decades of Belgian Marine Monitoring: uplifting historical data to today's needs - Final Report*.

Lindegren, M., Checkley, D. M., Koslow, J. A., Goericke, R., & Ohman, M. D. (2018). Climate-mediated changes in marine ecosystem regulation during El Niño. *Global Change Biology*, *24*(2), 796–809. https://doi.org/10.1111/gcb.13993

Litchman, E., de Tezanos Pinto, P., Edwards, K. F., Klausmeier, C. A., Kremer, C. T., & Thomas, M. K. (2015). Global biogeochemical impacts of phytoplankton: A trait-based perspective. *Journal of Ecology*, *103*, 1384–1396. https://doi.org/10.1111/1365-2745.12438

Litzow, M. A., & Ciannelli, L. (2007). Oscillating trophic control induces community reorganization in a marine ecosystem. *Ecology Letters*, *10*(12), 1124–1134. https://doi.org/10.1111/j.1461-0248.2007.01111.x

Lomartire, S., Marques, J. C., & Gonçalves, A. M. M. (2021). The key role of zooplankton in ecosystem services: A perspective of interaction between zooplankton and fish recruitment. *Ecological Indicators, 129,* https://doi.org/10.1016/j.ecolind.2021.107867

Lund-Hansen, L. C. (2004). Diffuse attenuation coefficients Kd(PAR) at the estuarine North Sea-Baltic Sea transition: Time-series, partitioning, absorption, and scattering. *Estuarine, Coastal and Shelf Science*, *61*, 251–259. https://doi.org/10.1016/j.ecss.2004.05.004

Lüskow, F., & Riisgård, H. U. (2018). In Situ Filtration rates of Blue Mussels (Mytilus edulis) Measured by an Open-Top Chamber Method. *Open Journal of Marine Science*, *08*(04), 395–406. https://doi.org/10.4236/ojms.2018.84022

Maar, M., Nielsen, G., Bolding, K., Burchard, H., & Visser, A. W. (2007). Grazing effects of blue mussel Mytilus edulis on the pelagic food web under different turbulence conditions. *Source: Marine Ecology Progress Series*, *339*, 199–213. https://doi.org/10.2307/24871782

Marzetz, V., Spijkerman, E., Striebel, M., & Wacker, A. (2020). Phytoplankton Community Responses to Interactions Between Light Intensity, Light Variations, and Phosphorus Supply. *Frontiers in Environmental Science*, *8*. https://doi.org/10.3389/fenvs.2020.539733

Monod, J. (1949). The growth of bacterial cultures. *Annual Review of Microbiology*, *3*, 371–394. http://dx.doi.org/10.1146/annurev.mi.03.100149.002103

Mortelmans, J., Deneudt, K., Cattrijsse, A., Beauchard, O., Daveloose, I., Vyverman, W., Vanaverbeke, J., Timmermans, K., Peene, J., Roose, P., Knockaert, M., Chou, L., Sanders, R., Stinchcombe, M., Kimpe, P., Lammens, S., Theetaert, H., Gkritzalis, T., Hernandez, F., & Mees, J. (2019a). Nutrient, pigment, suspended matter and turbidity measurements in the Belgian part of the North Sea. *Scientific Data*, *6*(1). https://doi.org/10.1038/s41597-019-0032-7

Mortelmans, J., Goossens, J., Amadei Martínez, L., Deneudt, K., Cattrijsse, A., & Hernandez, F. (2019b). LifeWatch observatory data: Zooplankton observations in the Belgian part of the North Sea. *Geoscience Data Journal*, *6*(2), 76–84. https://doi.org/10.1002/gdj3.68

Moser, S. C., Williams, S. J., & Boesch, D. F. (2012). Wicked challenges at land's end: Managing coastal vulnerability under climate change. *Annual Review of Environment and Resources*, *37*, 51–78. https://doi.org/10.1146/annurev-environ-021611-135158

Naselli-Flores, L., & Padisák, J. (2022). Ecosystem services provided by marine and freshwater phytoplankton. *Hydrobiologia*. https://doi.org/10.1007/s10750-022-04795-y

Nielsen, T. G., & Maar, M. (2007). Effects of a blue mussel Mytilus edulis bed on vertical distribution and composition of the pelagic food web. *Marine Ecology Progress Series*, *339*, 185–198. http://dx.doi.org/10.3354/meps339185

Nizzoli, D., Welsh, D. T., & Viaroli, P. (2011). Seasonal nitrogen and phosphorus dynamics during benthic clam and suspended mussel cultivation. *Marine Pollution Bulletin*, *62*, 1276–1287. https://doi.org/10.1016/j.marpolbul.2011.03.009

Nohe, A., Goffin, A., Tyberghein, L., Lagring, R., De Cauwer, K., Vyverman, W., & Sabbe, K. (2020). Marked changes in diatom and dinoflagellate biomass, composition and seasonality in the Belgian Part of the North Sea between the 1970s and 2000s. *Science of the Total Environment*, *716*. https://doi.org/10.1016/j.scitotenv.2019.136316

Ogilvie, S. C. (2000). Phytoplankton depletion in cultures of the mussel Perna canaliculus. *MSc. Thesis.*

Ogilvie, S. C., Ross, A. H., & Schiel, D. R. (2000). Phytoplankton biomass associated with mussel farms in Beatrix Bay, New Zealand. In *Aquaculture* (Vol. 181). http://dx.doi.org/10.1016/S0044-8486(99)00219-7

Otero, V., Pint, S., Deneudt, K., De Rijcke, M., Mortelmans, J., Schepers, L., Cabrera, P., Sabbe, K., Vyverman, W., Vandegehuchte, M., & Everaert, G. (2022). Pronounced seasonal and spatial variability in determinants of phytoplankton biomass dynamics along a near-offshore gradient in the southern North Sea. *Biogeosciences Discuss. (Preprint)*. https://doi.org/10.5194/bg-2022-11

Petersen, J. K., Nielsen, T. G., van Duren, L., & Maar, M. (2008). Depletion of plankton in a raft culture of Mytilus galloprovincialis in Ría de Vigo, NW Spain. I. Phytoplankton. *Aquatic Biology*, *4*(2), 113–125. https://doi.org/10.3354/ab00124

Prins, T. C., Smaal, A. C., & Dame, R. F. (1998). A review of the feedbacks between bivalve grazing and ecosystem processes. *Aquatic Ecology, 31,* 349-359. http://dx.doi.org/10.1023/A:1009924624259

Richard, M., Archambault, P., Thouzeau, G., & Desrosiers, G. (2006). Influence of suspended mussel lines on the biogeochemical fluxes in adjacent water in the Îles-de-la-Madeleine (Quebec, Canada). *Canadian Journal of Fisheries and Aquatic Sciences*, *63*, 1198–1213. https://doi.org/10.1139/F06-030

Rockström, J., Steffen, W., Noone, K., Persson, Å., Chapin, F. S. I., Lambin, E., Lenton, T. M., Scheffer, M., Folke, C., Schellnhuber, H. J., Nykvist, B., De Wit, C. A., Hughes, T., Van Der Leeuw, S., Rodhe, H., Sörlin, S., Snyder, P. K., Costanza, R., Svedin, U., … Foley, J. (2009). Planetary Boundaries: Exploring the Safe Operating Space for Humanity. *Ecology and Society*, *14*(2). http://www.ecologyandsociety.org/vol14/iss2/art32/

Slavik, K., Lemmen, C., Zhang, W., Kerimoglu, O., Klingbeil, K., & Wirtz, K. W. (2017). The large scale impact of offshore wind farm structures on pelagic primary productivity in the southern North Sea. *Hydrobiologia*. https://doi.org/10.1007/s10750-018-3653-5

Soetaert, K., & Herman, P. M. J. (2009). *A Practical Guide to Ecological Modelling: using R as a simulation platform*. Springer Science+Business Media.

Sterner, R. W. (2009). Role of Zooplankton in Aquatic Ecosystems. in *Encyclopedia of Inland Waters*, 678–688. Elsevier Inc. https://doi.org/10.1016/B978

Thomann, R. V., & Mueller, J. A. (1987). *Principles of surface water quality modeling and control*. Harper & Row, New York.

Van Ginderdeuren, K., Van Hoey, G., Vincx, M., & Hostens, K. (2014). The mesozooplankton community of the Belgian shelf (North Sea). *Journal of Sea Research*, *85*, 48–58. https://doi.org/10.1016/j.seares.2013.10.003

Vanhellemont, Q., & Ruddick, K. (2014). Turbid wakes associated with offshore wind turbines observed with Landsat 8. *Remote Sensing of Environment*, *145*, 105–115. https://doi.org/10.1016/j.rse.2014.01.009

Verhalle, J., & Van de Velde, M. (2020). *Something is moving at sea: The marine spatial plan for 2020-2026*. Belgian Federal Public Service: Health, Food Chain Safety and Environment.

VLIZ. (2021). *LifeWatch observatory data: nutrient, pigment, suspended matter and secchi measurements in the Belgian Part of the North Sea*. https://doi.org/10.14284/441

VLIZ. (2023). *LifeWatch observatory data: zooplankton observations by imaging (ZooScan) in the Belgian Part of the North Sea*. https://doi.org/10.14284/584

Wei, Y., Ding, D., Gu, T., Jiang, T., Qu, K., Sun, J., & Cui, Z. (2022). Different responses of phytoplankton and zooplankton communities to current changing coastal environments. *Environmental Research*, *215*. https://doi.org/10.1016/j.envres.2022.114426

Welschmeyer, N. A., & Lorenzen, C. J. (1985). Chlorophyll budgets: Zooplankton grazing and phytoplankton growth in a temperate fjord and the Central Pacific Gyres. *Limnology and Oceanography*, *30*(1), 1–21. https://doi.org/10.4319/lo.1985.30.1.0001

Wishner, K. F., Seibel, B. A., Roman, C., Deutsch, C., Outram, D., Shaw, C. T., Birk, M. A., S Mislan, K. A., Adams, T. J., Moore, D., & Riley, S. (2018). Ocean deoxygenation and zooplankton: Very small oxygen differences matter. *Science Advances, 4*. https://doi.org/10.1126/sciadv.aau5180

Yebra, L., Puerto, M., Valcárcel-Pérez, N., Putzeys, S., Gómez-Jakobsen, F., García-Gómez, C., & Mercado, J. M. (2022). Spatio-temporal variability of the zooplankton community in the SW Mediterranean 1992–2020: Linkages with environmental drivers. *Progress in Oceanography*, *203*. https://doi.org/10.1016/j.pocean.2022.102782

Appendix A: Nutrient-Phytoplankton-Zooplankton-Detritus (NPZD) equations

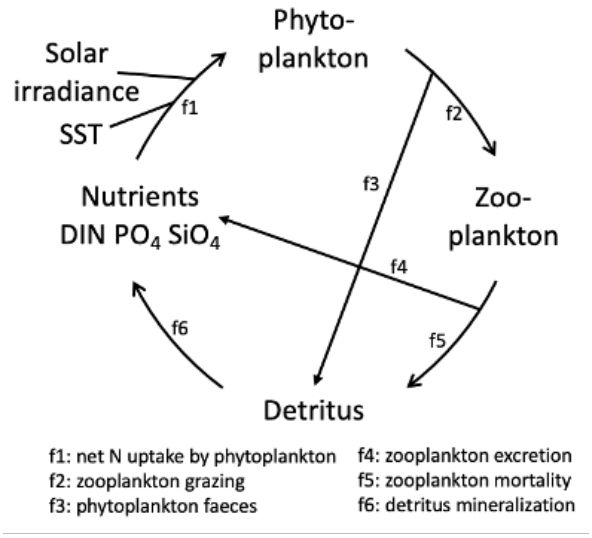

Figure A1: *Nutrient-Phytoplankton-Zooplankton-Detritus (NPZD) model structure*

Phytoplankton and zooplankton biomass was simulated from 2015-2017 using the NPZD ecosystem model created by Everaert et al. (2015) based on Soetaert en Herman (2009), and subsequently adjusted by Otero et al. (2022). The following equations determined the daily rates of change in the abundance phytoplankton (PHYTO), zooplankton (ZOO), and detritus (DET):

dPHYTO/dt = Nuptake (f1) - Grazing (f2)
dZOO/dt = Grazing (f2) - Faeces (F3) - Excretion (f4) - Mortality (f5)
dDET/dt = Mortality (F5) + Faeces (F3) - Mineralization (f6)

for which *t* indicates time in days.

Daily nutrient abundance is determined as the sum of *DIN*, PO_4 and SiO_4 based on the generalized additive models (GAM) for each. For a detailed description of GAM in this model, consult Otero et al. (2022).

NUTRIENTS = GAM (DIN) + GAM (PO_4) + GAM (SiO_4)

The model flows (Figure A1) were calculated as follows:

*Nuptake (f1) = maxUptake * PAR_lim * Temp_lim * P_lim * DIN_lim * Si_lim *PHYTO*
Grazing (f2) = maxGrazing (PHYTO/(PHYTO+ksGrazing))*ZOO*
*Faeces (f3) = pFaeces * Grazing*
*Excretion (f4) = excretionRate * ZOO*
*Mortality (f5) = mortalityRate * ZOO^2*
*Mineralization (f6) = 0.1*DET*

where *maxUptake*, *mineralizationRate*, *excretionRate*, *maxGrazing*, *ksGrazing*, *pFaeces* and *mortalityRate* are model parameters. And for which *Nuptake* is the phytoplankton nitrogen uptake, *PAR_lim* the limitation factor for photosynthetically active radiation (PAR), *Temp_lim* for sea surface temperature (SST), *P_lim* for PO_4, *DIN_lim* for DIN and *Si_lim* for SiO_4.

The limitation factors included in the previous equations were defined according to saturating Michaelis-Menten equations (Soetaert & Herman, 2009):

$$PAR\_lim = PAR/(PAR+ksPAR)$$
$$DIN\_lim = DIN /(DIN+ksDIN)$$
$$P\_lim = P/(P + ksP)$$
$$Si\_lim = Si/(Si + ksSi)$$

where *ksPAR*, *Tobs*, *ksDIN*, *ksP* and *ksSi* are parameters of the model.

The equation for PAR was defined based on the Lambert-Beer law (Kirk, 1994; Lund-Hansen, 2004):

$$PAR(f7) = I_0 e^{-Kd*z}$$

where I_0 is the surface irradiance (µEinst m^{-2} s^{-1}), z depth (m), and Kd the diffuse attenuation coefficient (m^{-1}).

Temperature limitation was described by a Thomann and Mueller equation (Thomann & Mueller, 1987)

$$Temp\_lim = \vartheta^{(Temp - Tobs)}$$
$$\vartheta = 1.185 - 0.00729*Temp$$

Model output for phytoplankton biomass is expressed in chlorophyll concentration. This was converted as follows:

$$Chlorophyll = chlNratio * PHYTO$$

In the mussel aquaculture scenario, the grazing equation itself was adapted to simulate mussel grazing on phytoplankton. This was done by adapting the grazing equation as follows:

$$Grazing\ (f2) = maxGrazing* (PHYTO/(PHYTO+ksGrazing))*(ZOO \mathbf{+ 0,081})$$

Note that an 'if…else' function from Base R ensured this constant would only be included when phytoplankton biomass was between 0.5 and mgL^{-1}.

All model calculations were performed in R (R Core Team, 2022; version 4.2.1) using the following packages:

- doParallel (Microsoft Corporation and Weston, 2020)
- dplyr (Wickham et al., 2020)
- foreach (Microsoft and Weston, 2020)
- ggplot2 (Wickham, 2016)
- ggpubr (Kassambara, 2019)
- lubridate (Grolemund and Wickham, 2011)
- parallel (R Core Team, 2018)
- plyr (Wickham, 2011)
- stats (R Core Team, 2018)
- viridis (Garnier, 2018)
- xts (Ryan and Ulrich, 2020)

Appendix B: Model spin-up time

In the mussel aquaculture and offshore wind farm scenarios variation was very high in 2014. This becomes clear when plotting the mean and standard deviation for the model simulations for each scenario (Figure B1). However, by 2015 the biomass predictions appear to be stabilized. This increased model spin-up time is likely due to the lack of model validation by comparison to *in situ* plankton biomass. Hence, 2015-2017 was selected for analysis in this thesis.

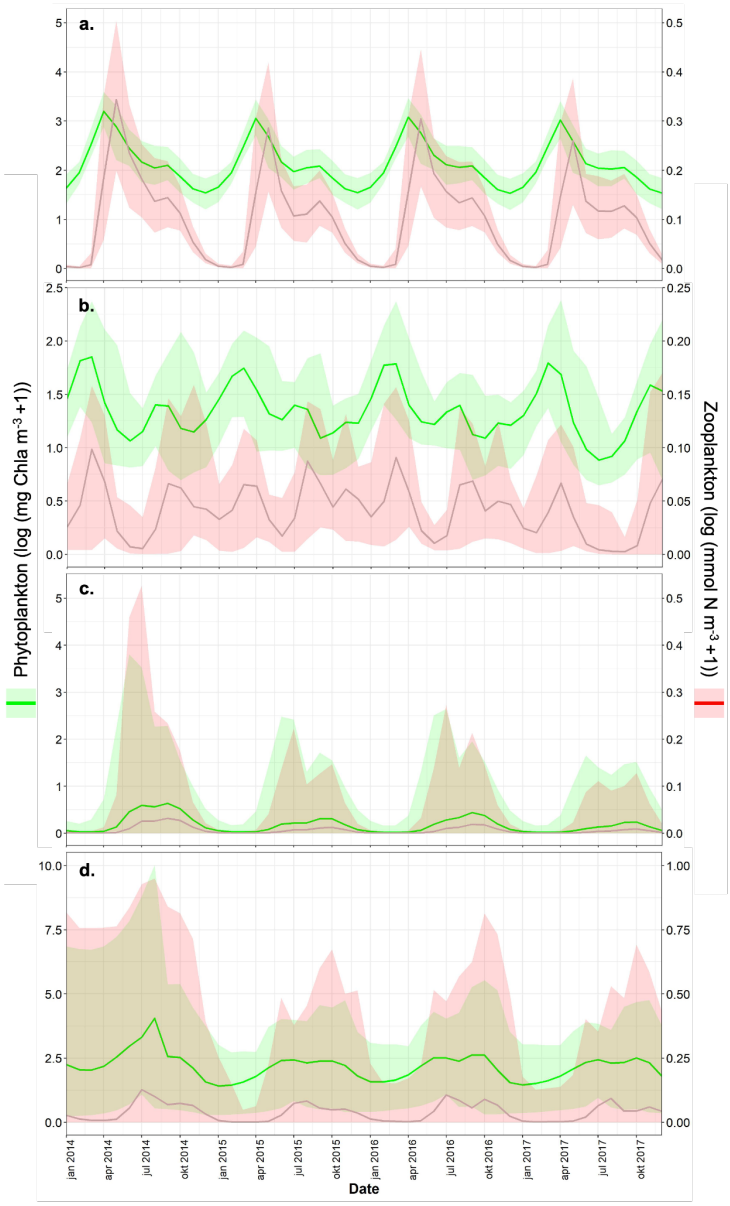

Figure B1: *Median and interquartile range for the model simulations of each scenario from 2014-2017: (a) nearshore baseline, (b) offshore baseline, (c) mussel aquaculture and (d) offshore wind farm.*